JCI The Journal of Clinical Investigation

Epithelial-mesenchymal transition leads to NK cell–mediated metastasis-specific immunosurveillance in lung cancer

Peter J. Chockley, … , Theodore J. Standiford, Venkateshwar G. Keshamouni

J Clin Invest. 2018. https://doi.org/10.1172/JCI97611.

Research Article In-Press Preview **Immunology** **Oncology**

During epithelial-mesenchymal transition (EMT) epithelial cancer cells trans-differentiate into highly-motile, invasive, mesenchymal-like cells giving rise to disseminating tumor cells. Only few of these disseminated cells successfully metastasize. Immune cells and inflammation in the tumor microenvironment was shown to drive EMT, but few studies investigated the consequences of EMT on tumor immunosurveillance. In addition to initiating metastasis, we demonstrate that EMT confers increased susceptibility to NK cells and contributes, in part, to the inefficiency of the metastatic process. Depletion of NK cells allowed spontaneous metastasis without effecting primary tumor growth. EMT-induced modulation of E-cadherin and cell adhesion molecule 1 (CADM1) mediated increased susceptibility to NK cytotoxicity. Higher CADM1 expression correlates with improved patient survival in two lung and one breast adenocarcinoma patient cohorts and decreased metastasis. Our observation reveal a novel NK-mediated, metastasis-specific, immunosurveillance in lung cancer and presents a window of opportunity for the prevention of metastasis by boosting NK cell activity.

Epithelial-Mesenchymal Transition Leads to NK Cell-mediated Metastasis-specific Immunosurveillance in Lung Cancer

Peter J. Chockley[1, 2], Jun Chen[1], Guoan Chen[3], David G. Beer[3], Theodore J. Standiford[1], and Venkateshwar G. Keshamouni[1]*

Division of Pulmonary and Critical Care Medicine, Department of Internal Medicine[1], Graduate Program in Immunology[2], Department of Surgery[3], University of Michigan, Ann Arbor, MI 48109.

Running Title: EMT confers susceptibility to NK-mediated cytotoxicity

***Address for Correspondence:** Venkateshwar G. Keshamouni, Ph.D, Division of Pulmonary and Critical Care Medicine, Department of Internal Medicine, University of Michigan Medical Center, 4062 BSRB, 109 Zina Pitcher Place, Ann Arbor, MI 48109, Phone: 734-647-9527, Fax: 734-615-2331, e-mail: vkeshamo@umich.edu*

Footnotes:

This research is funded by, NIH/NCI (CA132571-01) grant, and the Elizabeth A. Crary Fund to V.G.K. Rackham Graduate Experimental Research Grant, Rackham Graduate Pre-Doctoral Fellowship, Miller Award for Innovative Immunology Research, T32 AI007413 to P.J.C. Research reported in this manuscript was also supported by the NIH/NCI (P30CA046592) to UMCCC.

Conflict of interest
The authors have declared that no conflict of interest exists.

SUMMARY

During epithelial-mesenchymal transition (EMT) epithelial cancer cells trans-differentiate into highly-motile, invasive, mesenchymal-like cells giving rise to disseminating tumor cells. Only few of these disseminated cells successfully metastasize. Immune cells and inflammation in the tumor microenvironment was shown to drive EMT, but few studies investigated the consequences of EMT on tumor immunosurveillance. In addition to initiating metastasis, we demonstrate that EMT confers increased susceptibility to Natural Killer (NK) cells and contributes, in part, to the inefficiency of the metastatic process. Depletion of NK cells allowed spontaneous metastasis without effecting primary tumor growth. EMT-induced modulation of E-cadherin (E-cad) and cell adhesion molecule 1 (CADM1) mediated increased susceptibility to NK cytotoxicity. Higher CADM1 expression correlates with improved patient survival in two lung and one breast adenocarcinoma patient cohorts and decreased metastasis. Our observation reveal a novel NK-mediated, metastasis-specific, immunosurveillance in lung cancer and presents a window of opportunity for the prevention of metastasis by boosting NK cell activity.

Keywords: NK-ligands, CADM1, TGF-beta, E-cadherin, and lung cancer

INTRODUCTION

Significant progress has been made in determining and defining the key regulators of immunosurveillance in primary tumor, wherein the balance of pro-tumor and anti-tumor responses dictates tumor progression. Targeting these key regulators led to the successful development of check-point inhibitors that boost T-cell-mediated immunity against multiple tumor types, including non-small lung cancer (NSCLC) (1, 2). It is now increasingly clear that the microenvironment and the conditions tumor cells encounter in the primary tumor are disparate from what they encounter during metastasis. This suggests that mechanisms of immunosurveillance in the primary tumor may also be different from those that regulate metastatic spread (3) indicating the existence of metastasis-specific immunosurveillance (3-8).

Epithelial-mesenchymal transition (EMT) involves dissolution of cell-cell adhesions, down-regulation of epithelial markers, induction of mesenchymal markers, and breach of the basement membrane to migrate and invade (9, 10). In addition, EMT also endows cancer cells with stem cell-like properties, resistance to targeted therapies, and the ability to evade host immunosurveillance (11, 12). The multifunctional cytokine transforming growth factor-β (TGF-β) is a potent inducer of EMT and promotes tumor progression in late stage tumors (13). Consistently, expression of TGF-β is frequently up-regulated in cancers, including NSCLC (14), and is correlated with enhanced invasion, metastasis, and poor prognosis for patients with lung cancer (15). In NSCLC, we have shown that TGF-β-induced EMT confers a migratory and invasive phenotype promoting metastasis (16, 17), inhibition of EMT blocked tumor metastasis (18, 19), and an EMT-associated secretory phenotype was predictive of outcomes in NSCLC patients (20), demonstrating the biological and clinical significance of EMT in lung tumor progression.

Given the extensive molecular and cellular changes that occur during EMT, it is likely that tumor cell interactions with both innate and adaptive immune cells in the tumor microenvironment (TME) will be altered. Several studies implicated both innate and adaptive immune cells as drivers of EMT (21). However, few studies have investigated the immunomodulatory consequences of EMT (22). Studies to date have shown evasion of T-cell responses and suppression of dendritic cell functions by cells undergoing EMT, suggesting an important role for EMT in immune editing (23, 24). Consistent with this, we demonstrated an immune evasive consequence of EMT by which tumor cells escape complement dependent cytotoxicity by modulating the complement regulatory protein CD59 (25). In contrast, here we report a novel and unexpected consequence of EMT that confers enhanced susceptibility to Natural Killer (NK) cell-mediated killing.

NK cells are innate lymphoid cells known for their ability to recognize and rapidly eliminate infected or transformed cells (26-28). In humans, there is a correlation between low NK cell cytotoxicity in peripheral blood and increased cancer risk (29). Conversely, NK cell infiltration into tumor tissue is associated with better patient prognosis in multiple malignancies, including NSCLC (29). However, studies investigating their role in tumor progression and metastasis are very limited. NK cells express an array of germline-encoded receptors that enable them to detect and respond to their targets while sparing normal cells. Depending on the signal they transmit, these receptors are classified into inhibitory and activating receptors (30). Integration of signaling from these receptors determines whether or not an NK cell becomes activated. NK cells use their inhibitory receptors to detect the presence of major histocompatibility complex (MHC) class I as self-molecules on potential target cells. NK cells also express other non-MHC dependent inhibitory receptors, including killer lectin-like receptor G 1 (KLRG1) (31). The Type I, epithelial cadherin (E-cad) has been identified as an inhibitory ligand that engages KLRG1 in both mice and humans (32). The cell adhesion molecule 1

(CADM1), has been identified as an activating NK ligand and binds to the cytotoxic and regulatory T-cell-associated molecule (CRTAM) receptor on NK cells (33). CADM1 is identified as tumor suppressor and is frequently down regulated in multiple different malignancies (34, 35). Here, we demonstrate that EMT-induced CADM1 expression, along with the down regulation of E-cad, regulates NK-mediated, metastasis-specific, immunosurveillance.

RESULTS

EMT Differentially Regulates NK Ligands and Confers Enhanced Susceptibility to NK Cytotoxicity

NK cell reactivity is regulated by the balance of activating and inhibitory receptor engagement by ligands expressed on the target cells. Analysis of a previously obtained time course gene expression profile during TGF-β-induced EMT (17, 36), identified differential modulation of several NK activating ligands: in addition to the modulation of epithelial and mesenchymal markers. We observed a significant time-dependent induction of mRNA for NK-activating ligands PVR, CADM1, ULBP2 and ULBP4 (**Figure 1A**). Similarly, among the known inhibitory ligands, E-cad expression was significantly suppressed but there was no significant change in the expression of MHC-I in response to EMT. Collectively, the increased expression of activating ligands and decreased expression of inhibitory ligands in tumor cells undergoing EMT suggests a potential increased susceptibility to NK-mediated cytotoxicity. To test this, we assessed the susceptibility of a panel of human cancer cell lines to NK-mediated cytotoxicity before and after EMT. All cell lines were stimulated with TGF-β to induce EMT and then co-cultured with human NK cell line, NK92mi, to assess tumor cell specific killing by flow cytometry (**Figure 1B**). Consistent with the ligand expression profile, we observed a significantly increased susceptibility to NK-mediated cytotoxicity in EMT cells compared to the controls at all tumor-to-NK cell ratios tested (**Figure 1C-G**). The EMT-induced susceptibility to NK cells was not

specific to lung cancer cells, but was also observed in breast (**Figure 1F**) and colon (**Figure 1G**) cancer cells suggesting that it may be a more general phenomenon in response to EMT. Similarly, murine lung cancer cells also demonstrated increased susceptibility to NK-mediated cytotoxicity after EMT (**Supplemental Figure 1A**). In this case, CD45+, NK1.1+, CD3e- NK cells isolated from total splenic cells after overnight culture were used as effector cells against murine lung cancer cells 344SQ as targets.

To demonstrate that this increased cytotoxicity is not specific to NK92mi cell line, untouched human NK cells were isolated from PBMCs of healthy donors as effectors against EMT and control A549 cells as targets. The differential susceptibility between EMT and control A549 cells was also observed when primary PBMC derived NK cells were used as effectors (**Figure 1H**). K562 cells were used as positive controls to ensure cytotoxic capable NK cells were isolated. Next, to demonstrate the direct link between EMT and NK-mediated immunosurveillance in vivo, we induced EMT in A549-GFP cells as described earlier (19) and injected them into the tail vein of two groups of $RAG^{-/-}$ mice. In one group, NK cells were depleted with weekly anti-Asialo GM1 (ASGM1) treatment and mice were sacrificed after 6-8 weeks to assess lung metastasis. We observed metastatic lung nodules only in the mice treated with ASGM1 and not in the control group (**Figure 1I**), demonstrating EMT induced susceptibility to NK-mediated immunosurveillance, in vivo.

NK Cell Depletion Allows Spontaneous Metastasis Without Effecting Primary Tumor Growth

In earlier studies we demonstrated that TGF-β-induced EMT in A549 cells triggers a migratory and invasive phenotype in vitro and promotes metastasis in vivo (16, 19). Inhibition of TGF-β signalling, which prevents EMT, blocked metastasis of A549 cells (19) indicating an EMT-dependent metastasis model. To assess the role of NK cells in the above model, we

implanted 10^6 A549 cells in two groups of RAG1$^{-/-}$ mice on either side of the dorsal flank. RAG1$^{-/-}$ mice do not have T and B cells but have functional NK cells. One group of mice were treated weekly with ASGM1 antibody to deplete NK cells. Interestingly, depletion of NK cells had no effect on the primary tumor growth (**Figure 2A**). In contrast, we observed spontaneous lung metastasis only in the mice that are depleted of NK cells **(Figure 2B**), suggesting the presence of an NK-mediated metastasis-specific immunosurveillance. Together with the observations in (**Figure 1**), this also suggests an EMT-dependent mechanism. To assess the extent of depletion, splenic cells were isolated and analysed by flow cytometry. We observed nearly a 90% reduction in the number of NK cells (CD45+/NK1.1+/CD3e- cells) with ASGM1 treatment (**Supplemental Figure 2B**).

To assess the role of NK cells in metastasis in an immunocompetent host, we employed a syngeneic murine model of Lewis lung carcinoma (LLC) cells. We subcutaneously implanted LLC cells in C57BL/6 hosts with and without NK cell depletion using ASGM1 antibody. LLC cells grow very aggressively in the syngeneic host but do not metastasize. Similar to the xenograft model above, depletion of NK cells had no effect on the primary tumor growth (**Figure 2C**), but we observed spontaneous lung metastasis only in mice that were treated with ASGM1 antibody **(Figure 2D**). In a parallel experiment, we used NK1.1 antibody instead of ASGM1 to deplete NK cells and observed similar results (**Supplemental Figure 3 A and B**). Since there is no single method that can exclusively deplete only NK cells, our data with ASGM1 (which is also known to effect basophil populations) and NK1.1 Ab (which is also known to deplete NK-T cells) showing similar effects demonstrate a NK cell-dependent phenomena.

The potential contribution of T and B cells to the observed metastasis-specific immunosurveillance was assessed by implanting LLC cells in T and B cell deficient RAG$^{-/-}$ mice. Notably, we observed similar spontaneous metastasis only upon NK depletion (**Figure 2F**), and there was no effect on the growth of the primary tumor with and without NK cell depletion

(**Figure 2E**). We also observed similar results when 344SQ cells were implanted in C57BL/6 mice with and without ASGM1 NK depletion (**Supplemental Figure 1 C and D**). Collectively, similar observations in four different models above demonstrate the presence of a NK cell-dependent, metastasis-specific immunosurveillance mechanism.

Loss of E-Cadherin Expression Sensitizes Tumor Cells to NK Cytotoxicity Through KLRG1

Classically, inhibitory signals on NK cells are mediated by receptors that recognize MHC-I molecules. However, recent studies demonstrate that NK cells also express other receptors like KLRG1 that can recognize MHC-independent inhibitory signals such as E-cad (32). Since E-cad is down regulated during EMT with a concomitant increase in the susceptibility to NK cell-mediated cytotoxicity, we reasoned that E-cad may be an important inhibitory signal that protects epithelial cells from NK cell mediated cytotoxicity. To test this, we inhibited E-cad expression by three different siRNA molecules in A549 (**Figure 3A**), before assessing their susceptibility to NK cell cytotoxicity using NK92mi cells as described for Figure 3. We observed that E-cad inhibition increased susceptibility to A549 cells to NK-mediated cytotoxicity (**Figure 3B**). However, the magnitude of cytotoxicity did not reach the levels of observed after EMT. Next, we determined whether E-cad-induced inhibitory signaling is indeed mediated through KLRG1 on NK cells. siRNA-mediated inhibition of KLRG1 expression in NK92mi cells (**Figure 3C**) enhanced their cytotoxicity against the non-EMT control as well as EMT induced tumor cells (**Figure 3D**) demonstrating that KLRG1 mediates E-cad-induced inhibitory signaling. Inhibiting the E-cad/KLRG1 axis did not fully recapitulate the enhanced cytotoxicity against A549 cells undergoing EMT, suggesting that it may also require the induction of an activating ligand.

NKG2D Receptor is Not Involved in the EMT-induced Susceptibility to NK-Mediated Cytotoxicity

Since we observed a robust induction of NKG2D ligands ULBP2 and ULBP4 during EMT, we tested the potential involvement of NKG2D as an activating NK cell receptor mediating tumor cell killing after EMT. We assessed the involvement of NKG2D by independently blocking its expression, using siRNA, and function, using neutralizing antibodies, in NK92mi cells. K562 cells, whose NK-mediated cytotoxicity is partly NKG2D dependent, were used as a positive control (37). Interestingly, inhibition of expression or function of NKG2D receptors had no effect on A549 tumor cell killing before or after EMT (**Figure 4 A and B**). This suggests that alternative activating receptors may be critical for NK cell recognition of A549 cells post-EMT.

CADM1 Expression is Modulated by EMT-MET Cycling and Mediates Tumor Cell Susceptibility to NK Cytotoxicity

Given that neutralizing NKG2D receptors had no effect, we tested the role of CADM1, the next most abundant NK ligand induced during EMT, as a potential activating ligand mediating EMT-induced susceptibility to NK cells. CADM1, also known as TSLC1, is identified as a tumor suppressor in lung cancer and its expression is frequently lost in 40% of NSCLC. (34, 38, 39). Interestingly, CADM1 was also shown to form heterophillic interactions with an immunoglobulin family receptor known as CRTAM that serves as its cognate receptor and expressed on activated NK cells, suggesting a role for CADM1 in immunosurveillance (33). We observed a robust modulation of CADM1 protein in response to TGF-β-induced EMT-MET cycling along with the epithelial (E-cad) and mesenchymal markers (Vim) in a time-dependent fashion (**Figure 5A**). We further validated TGF-β-induced CADM1 expression with concomitant down regulation of E-cad by immunofluorescence (**Figure 5B**).

To determine the role of CADM1 in NK-mediated cytotoxicity, we developed stable A549 cells with CADM1 knockout by genome editing using CRISPR-Cas9 technology along with constitutive mCherry expression (A549-CADM1 KO) together with corresponding non-targeting control cell line (A549-NT) (**Figure 5C**) and assessed the susceptibility, before and after EMT, to NK cell cytotoxicity. We observed that CADM1 inhibition abrogated EMT-induced susceptibility of A549 cells to NK92mi cytotoxicity (**Figure 5D**) as well as to the primary donor-derived NK cell cytotoxicity (**Figure 5E**). Together with E-cad data (**Figure 3**), this demonstrates that modulation of both E-cad and CADM1 expression can regulate tumor cell susceptibility to NK-mediated cytotoxicity. Analysis of E-cad and CADM1 expression in primary A549 tumors from Figure 2A (**Supplemental Figure 4 A and B**) showed no difference with or without NK cell depletion; which is consistent with lack of effect on primary tumor growth kinetics. Together with analysis of E-cad and CADM1 expression in susceptibility cell lines (**Supplemental Figure 5**) further suggests that potentially it is the ratio between E-cad and CADM1 that dictates susceptibility to NK-mediated cytotoxicity. Interestingly, CADM1 knockout had no effect on TGF-β-induced EMT (**Supplemental Figure 6**).

Inhibition of CADM1 in Tumor Cells Enables Immune Evasion and promotes Metastasis

To assess the impact of CADM1 inhibition on tumor metastasis, we implanted A549-CADM1 KO and A549-NT cells in to the dorsal flanks of $RAG1^{-/-}$ mice and assessed primary tumor growth and lung metastasis. Notably, there was no difference in the kinetics of primary tumor growth between A549-CADM1 KO and A549-NT due to CADM1 inhibition (**Figure 6A**). As expected, the tumors from the control A549-NT cells did not metastasize. However, there was a striking increase in overt lung metastasis from A549-CADM1 KO cells even without NK cell depletion, as assessed by gross counting (**Figure 6B**) and visualizing mCherry positive tumor cell colonies in the lung (**Figure 6C**). This indicates CADM1 inhibition alone is sufficient to

allow metastasis which is otherwise blocked by NK cell immunosurveillance. Putatively, loss of CADM1 observed in various cancers may be an immune evasive strategy employed by tumors.

Restoring CADM1 Expression in Tumor Cells is Sufficient to Confer Susceptibility to NK Cytotoxicity

It is well documented that CADM1 expression is frequently lost in 40% of lung cancers either due to promoter hypermethylation, or loss of heterozygosity (LOH) (35). Here we tested the efficacy of two approaches of restoring CADM1 expression on NK-mediated cytotoxicity. First, in A549 cell line with LOH for CADM1, we generated a stable cell line expressing a doxycycline (dox)-inducible CADM1 (A549-CADM1 OE). Dox-induced overexpression of CADM1 had no effect on the growth and on the TGF-β-induced EMT in A549-CADM1 OE cells (**Supplemental Figure 7**). However, dox-induced CADM1 overexpression alone was sufficient to confer susceptibility to NK-mediated cytotoxicity, without the induction of EMT (**Figure 7A**). Similarly, in a cell line with CADM1 promoter hypermethylation (H1299) (40), we were able to restore CADM1 expression by culturing H1299 cells in the presence of 5'-azadeoxycytidine (5-aza), a pan-demethylating agent, for 6 days **(Figure 7B**). Consistent with the restored CADM1 expression, 5-aza treatment also rendered H1299 cells susceptible to NK-mediated cytotoxicity (**Figure 7B**). The efficacy of above two methods demonstrates that restoring CADM1 expression can be a potential immuno-therapeutic strategy for lung cancer.

CADM1 Expression in Primary Tumor Correlates with Improved Patient Survival and Decreased Metastasis

To further demonstrate the clinical significance, gene expression of CADM1 was assessed in a primary human lung adenocarcinoma data-set (n=442) (41). Univariate Cox overall survival analysis revealed increased expression of CADM1 strongly correlated with prolonged patient survival (**Figure 8A**). CADM1 expression inversely correlated with higher

tumor stage and positive nodal status (**Figure 8B and 8C**). We further validated the survival analysis in an independent lung adenocarcinoma data set (n=720) (**Figure 8D**)(42), and also in a ER+ breast cancer data set (n=548) (**Figure 8E**) (43) as we saw an enhanced EMT-induced NK cytotoxicity in MCF7, a ER+ breast cancer cell line (**Figure 1F**). In all cases we observed similar survival benefit with increasing CADM1 expression. Additionally, we investigated the correlation between E-cad expression and patient survival in the same cohorts and found no effect on patient outcome, (**Supplemental Figure 8**). This observation is consistent with the modest effect of E-cad/KLRG1 inhibition (**Figure 3**) on NK cytotoxicity, indicating the need of an activating ligand for optimum NK activation.

DISCUSSION

Studies thus far have focused on understanding how a small proportion of disseminating cells escape host surveillance and metastasize. Unfortunately, very little attention is paid to the understanding of the mechanisms which successfully eradicate more than 99% of tumor cells. It is now increasingly appreciated that the immune system plays an important role in the surveillance against metastasis (3-7). Since EMT is critical for metastasis, exclusive focus on evasive or resistance mechanisms that cells acquire after EMT may have promoted an unintended bias; that cells undergoing EMT must be resistant to host anti-tumor responses. On the contrary, it is equally feasible that metastatic cells after EMT are also vulnerable to host immunosurveillance. In other words, when cancer cells exit the immunosuppressive primary tumor microenvironment it is possible that they may pay a toll to metastasize by becoming more susceptible to host immunosurveillance. Strongly supporting the above notion, our studies show that in addition to promoting an invasive phenotype (18, 19, 44), EMT renders cancer cells more susceptible to NK-mediated killing, in vitro, by modulating activating and inhibitory ligands. This is consistent with a singular in vitro study that showed increased susceptibility of a colon cancer cell line to NK cells (45). More importantly, for the first time, we demonstrated the consequence

of this enhanced susceptibility on tumor metastasis in vivo in multiple mouse models. In addition, we also observed this phenomenon with breast cancer cell lines indicating the broader significance of this study. Together, this suggests that the NK cell-mediated immunosurveillance mechanism may contribute in part to the inefficiency of the metastatic process.

To date, a significant number of studies in mouse models have implicated NK cells in the control of metastasis (46) and also showed that evasion of NK-mediated immunosurveillance plays a critical role in maintaining metastatic latency (47). Supporting this, clinical studies in multiple solid tumors demonstrated an inverse correlation between the number of circulating or tumor-infiltrating NK cells and the presence of metastasis at the time of diagnosis (46). Similarly, higher expression of NK cell activating receptors was shown to correlate with better prognosis in patients with or at the risk of metastasis. However, mechanisms involved in this metastasis-specific control are unknown. Our current observations are not only consistent with the above notion but also provide a mechanistic basis by determining the activating and inhibitory axis involved. Moreover, we did not observe any effect of NK cell depletion on the growth of the primary tumors. TGF-β is known to inhibit NK cell function (48, 49) and the TGF-β-rich TME may explain why NK cell depletion has no effect on the primary tumor growth. However, TGF-β levels in circulation or at the site of metastasis are substantially lower than in the primary TME, enabling metastasis-specific immunosurveillance. An earlier study demonstrated that EMT allows cancer cells to escape T cell immunosurveillance (23) and enable them to leave the primary tumor. Whereas, our data suggests that concomitant modulation of NK ligands due to EMT will make them vulnerable to NK-mediated cytotoxicity as they abandon the immunosuppressive primary TME: thereby, allowing metastasis-specific control.

The direct interaction between KLRG1 and E-cad has been established. It is implicated in the recognition of non-MHC ligand mediated inhibitory signaling in NK cells (32). Even though the role of this interaction has been proposed in tumor progression, it has never been

demonstrated in a physiologically relevant context, until this study. Our data suggests that the ratio between the E-cad and the CADM1 expression may dictate the susceptibility of tumor cells to NK-mediated cytotoxicity. In the case of CADM1, its tumor suppressor activity has been attributed to its cell adhesion functions through homophilic interactions, mediated by its C-terminal intracellular domain and downstream membrane associated guanylate kinases (MaGUK) (50, 51). The role of CADM1 in the evasion of immunosurveillance has never been considered as potential mechanism for tumor suppression. Earlier studies that demonstrated the inhibition of tumor growth by CADM1 overexpression were carried out in nude mice or mice that carry functional NK cells and overlooked the role of NK cells in the observed tumor suppression (34, 52-54). Our data clearly demonstrates that CADM1 overexpression is sufficient to make cancer cells sensitive to NK cells, in vitro. Therefore, to assess the growth of CADM1 overexpressing cells in the presence and absence of NK cells may clarify the mechanism by which CADM1 exerts its tumor suppressive activity.

One limitation of our study is we still do not know at which step(s) of the metastatic cascade NK cells operate to control metastases. To address this, it is important to investigate the effect of NK cell depletion on various steps of metastatic cascade including, local invasion, intravasation, CTC persistence, extravasation and survival at the distant site. Animal models that allow for the precise monitoring of each of the above steps are essential to adequately address the above question. Although NK cells were the focus of this study, it is important to investigate the role of other immune cells in the control of metastasis, either in conjunction or independent of NK cells. The role of cytotoxic T-cells might be particularly important as sub-populations as these cells also express KLRG1 and CRTAM receptors that recognize E-cad and CADM1 (55, 56).

In summary, contrasting the prevailing notion that EMT confers only tumor promoting functions in cancer cells, this study strongly suggest that EMT also renders cancer cells more

susceptible to NK cell cytotoxicity and contributes to the inefficiency of metastasis. This novel metastasis-specific immunosurveillance mechanism presents a potential window of opportunity for the prevention of metastasis by boosting NK cell functions. Multiple NK based therapeutic strategies, both at preclinical and clinical stage, are under development for cancer immunotherapy with promising outcomes (57, 58). Approaches that can induce or restore activating ligands or that can neutralize inhibitory ligands or receptors may boost NK cell functions. Analogous to CAR-T cells, these approaches can also aid in the design of “super-NK” cells for cancer immunotherapy.

METHODS

Cell lines and culture conditions

Murine Lewis Lung Cancer (LLC) and (344SQ) and human: A549, NK92mi, H1299, H460, H358, K562, NK92mi and MCF7 cells were grown in 95%air/%5 CO_2 at 37° Celsius. Culture media for LLC cells is Dulbecco's Modified Eagle Medium (DMEM) supplemented with 10% heat-inactivated fetal bovine serum (FBS), 0.3 mg/mL L-glutamine, 50 U/mL penicillin, and 50 µg/mL streptomycin. Human cell lines were cultured according to the guidelines listed from the American Type Culture Collection (ATCC). For EMT experiments, cells were grown in 6-well plate in 30–40% confluency (50,000 cells/well) in complete medium. They were serum starved for 24hrs and then treated with TGF-β (5ng/ml) for 72hrs.

Mice

8-week-old male or female C57BL/6J, B6.129S7-*Rag1*^{tm1Mom}/J (RAG1$^{-/-}$) mice were purchased from Jackson Laboratory and housed in SPF conditions. All animal experiments were conducted in accordance with procedures approved by the University Committee on Use and Care of Animals and conformed to the policies and procedures of the Unit for Laboratory Animal Medicine at the University of Michigan.

Tumor Models

Cancer cells were grown in their respective media. Cells were lifted using EDTA and removed with complete media. Cells were spun at 250g in a table top centrifuge and washed 2 times with plain serum free media. Cells were then resuspended in plain media at $10x10^6$ cells per milliliter of media and stored on ice until injection.

Subcutaneous: Cells were loaded into a 1mL syringe fitted with a 26 gauge needle and 100uL of this cell suspension was injected subcutaneously in the right and left dorsal flanks of mice resulting in 2, $1x10^6$ cells injections per mouse. Tumors were measured twice weekly with manual calipers and the modified ellipsoidal volume equation was used $(LxW^2)/2$=Volume to determine tumor sizes. Mice were euthanized upon reaching a $2500mm^3$ tumor volume limit.

Experimental Metastasis: Cells were grown and lifted via EDTA, washed twice in DPBS and resuspended at $5x10^6$ cells per milliliter of DPBS. 200uL of this cell suspension was injected via lateral tail vein of mice. Mice were monitored and after 8 weeks mice were euthanized and lungs were excised for lung module counts.

In all models, lungs and primary tumors were excised and fixed with ice-cold 4% paraformaldehyde overt lung metastases were counted under magnifying glass. Additionally, lungs were cryoprotected in 30% sucrose solution, embedded in OCT, frozen, and sectioned at 10 micron thicknesses on a cryostat (Leica). These sections were then mounted with Prolong Gold AntiFade with DAPI (Thermofisher, CAT#P36931) and observed on an epiflourescent microscope.

siRNA Transfection

CDH1, KLRG1, NKG2D, CADM1 siRNA molecules were purchased from Integrated DNA Technologies. A scrambled sequence from the same company was used as control. Cells at 30–40% confluent (50,000 cells/well) were transfected with siRNA using Lipofectamine 2000 and OptiMEM medium. After 6 hours of transfection, cells were allowed to recover overnight

from transfection in RPMI-1640 medium with 10% FBS before inducing EMT or further assessments as indicated. NK92mi cells, 10^6, were transfected in a 5ml round bottom tubes.

Doxycycline inducible CADM1 gene expression

CADM1 cDNA approximately 1362bp was created using these two primers

5’ GGGCGGCCGCCAGGTGCCCGACATGGC 3’ NotI containing N-terminal

5’ AAGGAAAAAAGAATTCCAGTTGGACACCTCATTGAA 3’ EcoRI containing C-Terminal

Annealing temperature 65° Celsius, 35 cycles, 40 second annealing time, 90 second extensions using Promega GoTaq green mastermix, CAT# M7122, primer concentration were 1uM each. Lentiviral pLVX-TRE3g and pLVX-TET3g plasmids, CAT#631187, Clontech, were used to create stable doxycycline inducible cell lines. pLVX-TRE3g was cut with EcoRI-HF,CAT#R3101S, and NotI-HF, CAT#R3189S, New England Biolabs Inc, restriction enzymes. These same enzymes were used to cut the PCR CADM1 product overnight and were subsequently heat inactivated and gel purified in 2% agarose and visualized with ethidium bromide for 1hour at 110V. Bands were excised and purified using Qiagen Gel Extraction Kit, CAT#28704. Vector and insert were combined at a 1:3 ratio and ligated overnight at ~16° Celsius using T4 DNA ligase, CAT#M0202T, New England Biolabs Inc.

Ligation reactions were transformed into One Shot STBL3 E.Coli cells, CAT# C737303, ThermoFisher Scientific, via heat shock for 42 seconds and plated on ampicillin 100ug/mL agar plates overnight. Colonies were isolated in 20uL LB media and PCR was performed to initially screen for CADM1 cDNA expression. Positive colonies were then grown overnight in 5mL LB media containing 100ug/mL ampicillin plasmids were purified using QIAprep Spin, CAT#27104, Qiagen.

Purified plasmids were digested with EcoRI and NotI and gel electrophoresed plasmids containing inserts were sequenced using MSCV reverse primer.

5’ CAGCGGGGCTGCTAAAGCGCATGC 3’

Sequencing was performed at the University of Michigan Sequencing Core.

Sequence validated plasmids were then utilized in lentiviral production.

Lentiviral Particles were made at the University of Michigan Vector Core **Cancer Center (P30 CA046592)**

CRISPR/Cas9 Mediated Deletion

A549 expressing Cas9 cells were purchased from Genecopiea CAT#SL504. Signal guide RNAs were also purchased from Genecopiea. CADM1, CAT# HCP206321-LvSG03-3-B, and NT, CAT# CCPCTR01-LvSG03-B, these bacterial stocks were plated and a single colony was selected for plasmid growth and subsequent virus production. Lentiviral particles containing the specific targeting constructs were then used to infect A549-Cas9 cells. These new cell lines were verified by puromycin selection 1ug/ml and mCherry expression validated by flow cytometry.

Western Blot Analysis

Cells were washed with dulbecco’s Phosphate Buffered Saline (DPBS), pH 7.4, after treatment and lysed in radio immunoprecipitation assay buffer (RIPA) containing NaF, Na3Vo4 and protease inhibitor. Samples containing10-20µg of total protein were electrophoresed on SDS-polyacrylamide gels and transferred onto a polyvinyldifluoride membrane by electro-blotting. Membranes were probed with primary antibodies.

Anti-CADM1(3E1), CAT# CM004-3, MBL, 1:1000

Anti-CADM1(polyclonal), CAT# ABT66, EMD Millipore 1:500

Anti-SynCAM(polyclonal), CAT#S4945, Sigma-Aldrich, 1:1000

Anti-E-Cadherin(36/E-Cadherin), CAT# 610182, BD Transduction Laboratories 1:1000

Anti-N-Cadherin(32/E-Cadherin), CAT# 610921, BD Transduction Laboratories 1:1000

Anti-GAPDH-HRP(GAPDH 71.1), CAT# G9295, Sigma-Aldrich 1:10,000

Anti-Vimentin (13.2) CAT# V5255, Sigma-Aldrich, 1:1000

Secondary Antibodies containing horseradish peroxidase(HRP)

Anti-Mouse-HRP(polyclonal), CAT#A9044, Sigma –Aldrich, 1:80,000

Anti-Chicken HRP(polyclonal), CAT#31401 , Thermofisher 1:10,000

Immunodepletion

The following antibodies were administered i.p. to deplete NK cells; per mouse: 25 µL of stock rabbit polyclonal anti-asialo GM1(ASGM1), cat. no. 986-10001, Wako, diluted to a final volume of 100 µL in DPBS. 200ug murine monoclonal anti-NK1.1 (clone:PK136), CAT# BP0036, BioXcell, diluted to a final volume of 100uL in ddH2O. 100 µL of undiluted normal rabbit serum (NRS), CAT# 16120, Life Technologies, was used as the control for ASGM1. 200ug murine monoclonal anti-IgG2A (clone:C1.18.4), CAT# BP0085, BioXcell, diluted to a final volume of 100uL in ddH2O was used as the control for anti-NK1.1.

Flow cytometry

Cells were collected and spun at 250g and resuspended in FACS buffer(DPBS with 1% BSA) Non-specific antibody binding was blocked with either CD16/32 for mouse or 5% human serum for 10 minutes at room temperature. Cells were spun and washed in FACS buffer. Primary antibody incubations were performed at indicated dilutions for 30 minutes on ice. CD3e(145-2C11) 1:200, NK1.1(PK136) 1:100, CD45(30-F11) 1:200 BD Biosciences. KLRG1(13F12F2),

1:100, eBioscience. Cells were analyzed with an Attune Acoustic Flow cytometer (Applied Biosystems, Carlsbad, CA)

Sorting was performed on a FACS ARIA IIIu at the University of Michigan Flow cytometry core.

Analysis was performed with FlowJo version 10, FlowJo, LLC.

Human Natural Killer Cell Isolation

Human NK cells were isolated in an untouched manner using a commercially available MACS NK isolation Kit, Miltenyi Biotec, CAT#130-092-657. This was performed to the manufacturer's specifications. Briefly, donated peripheral blood samples from healthy donors were subjected to ACK red blood lysis and white blood cells were collected by centrifugation. Cells were counted and appropriate amounts of antibody cocktail were added from the NK isolation kit.

Cytotoxicity Assay

Target cells were cultured and treated with TGFβ (5ng/mL) in 1% serum media for 3 to 12 days, depending on cancer cell type as previously described. These cells were then lifted with EDTA , washed in DPBS, and labeled with carboxyfluorescein diacetate succinimidyl ester (CFSE) at 0.5uM concentration for 10 minutes. The staining was stopped with ice-cold complete media for 5 minutes, spun at 250g, and washed twice. Cells that were already GFP or mCherry positive were not stained and immediately used. These cells were counted and co-cultured for 4 hours with NK92mi killer cells in complete media corresponding to the cancer cells. These reaction tubes were then placed on ice after 4 hours and Propidium Iodide(PI) was added to a final concentration of 100ug/mL or Sytox Blue(Thermofisher, CAT#S34857) and incubated for 5 minutes and then analyzed via flow cytometry. Cells that were labelling dye or fluorophore positive and PI or Sytox Blue positive were considered dead and to determine the NK specific lysis the spontaneous death from cultures lacking NK cells were subtracted.

Immunocytochemistry/Immunohistochemistry

Cells were grown on glass coverslips, after treatments cells were fixed with ice-cold methanol for 15 minutes at -20 degrees Celsius. Cells were labelled with anti-E-cadherin(36/E-cadherin) conjugated with FITC, BD Transduction Laboratories, or with CADM1(ABT66) EMD millipore with subsequent anti-rabbit Alexa-488(R37116) secondary. Cells were mounted with Prolong Gold Antifade with DAPI and observed under a Nikon Eclipse Ti epifluorescent microscope. Primary tumor sections were immunolabeled with with anti-E-cadherin(36/E-cadherin) conjugated with FITC, BD Transduction Laboratories, or with anti-SynCAM(S4945) Sigma-Aldrich with subsequent anti-rabbit Alexa-488(R37116) secondary.

Statistical Analysis

All statistics were performed in Graphpad 6 from Prism. Violin plots were created in R with ggplot2 package, Version 1.0.143, RStudio, Inc. Heatmaps were generated with Morpheus, (https://software.broadinstitute.org/morpheus/). Metastatic quantifications were analyzed with a Mann Whitney U test. All survival analyses are Kaplan-Meier Survival Curves with Mantel-Cox Log Rank. Multiple group analyses were performed with a One-Way ANOVA with Tukey's post-hoc analysis. All other statistics are unpaired, two-tailed, student's t tests. Significance is delineated by *p<.05, **p<.01, ***p<.001, ****p<.0001 and mean±SEM is shown.

Study Approval

All animal experiments were approved by the IACUC of the University of Michigan and performed according to NIH guidelines. Blood samples were obtained with written and informed consent under IRBMED #HUM00075841 from the University of Michigan.

Contributions

P.J.C. and J.C performed experiments; P.J.C and V.G.K. designed experiments, analyzed data and wrote the manuscript; V.G.K supervised the study; D.G.B., G.C and T.J.S. gave reagents, analyzed data, and reviewed the manuscript; G.C helped with in-silico analysis.

Acknowledgements

We would like to thank S. Kunkel, C. Bonifant, R. Vittal, and C. Lumeng for reagents. B. Moore and M. Schaller for helpful comments and critiques. M. Newstead for lab support.

References

1. Ott PA, Hodi FS, and Robert C. CTLA-4 and PD-1/PD-L1 blockade: new immunotherapeutic modalities with durable clinical benefit in melanoma patients. *Clin Cancer Res.* 2013;19(19):5300-9.
2. Romano E, and Romero P. The therapeutic promise of disrupting the PD-1/PD-L1 immune checkpoint in cancer: unleashing the CD8 T cell mediated anti-tumor activity results in significant, unprecedented clinical efficacy in various solid tumors. *Journal for immunotherapy of cancer.* 2015;3(15.
3. Slaney CY, Rautela J, and Parker BS. The emerging role of immunosurveillance in dictating metastatic spread in breast cancer. *Cancer research.* 2013;73(19):5852-7.
4. Hong H, Gu Y, Zhang H, Simon AK, Chen X, Wu C, Xu XN, and Jiang S. Depletion of CD4+CD25+ regulatory T cells enhances natural killer T cell-mediated anti-tumour immunity in a murine mammary breast cancer model. *Clinical and experimental immunology.* 2010;159(1):93-9.
5. Olkhanud PB, Baatar D, Bodogai M, Hakim F, Gress R, Anderson RL, Deng J, Xu M, Briest S, and Biragyn A. Breast cancer lung metastasis requires expression of chemokine receptor CCR4 and regulatory T cells. *Cancer research.* 2009;69(14):5996-6004.
6. Paolino M, Choidas A, Wallner S, Pranjic B, Uribesalgo I, Loeser S, Jamieson AM, Langdon WY, Ikeda F, Fededa JP, et al. The E3 ligase Cbl-b and TAM receptors regulate cancer metastasis via natural killer cells. *Nature.* 2014;507(7493):508-12.
7. Yang L, Huang J, Ren X, Gorska AE, Chytil A, Aakre M, Carbone DP, Matrisian LM, Richmond A, Lin PC, et al. Abrogation of TGF beta signaling in mammary carcinomas recruits Gr-1+CD11b+ myeloid cells that promote metastasis. *Cancer Cell.* 2008;13(1):23-35.
8. Bidwell BN, Slaney CY, Withana NP, Forster S, Cao Y, Loi S, Andrews D, Mikeska T, Mangan NE, Samarajiwa SA, et al. Silencing of Irf7 pathways in breast cancer cells promotes bone metastasis through immune escape. *Nat Med.* 2012;18(8):1224-31.
9. Thiery JP, and Sleeman JP. Complex networks orchestrate epithelial-mesenchymal transitions. *Nature reviews Molecular cell biology.* 2006;7(2):131-42.
10. Tarin D, Thompson EW, and Newgreen DF. The fallacy of epithelial mesenchymal transition in neoplasia. *Cancer research.* 2005;65(14):5996-6000; discussion -1.
11. Zavadil J, Haley J, Kalluri R, Muthuswamy SK, and Thompson E. Epithelial-mesenchymal transition. *Cancer research.* 2008;68(23):9574-7.
12. Shibue T, and Weinberg RA. EMT, CSCs, and drug resistance: the mechanistic link and clinical implications. *Nature reviews Clinical oncology.* 2017;14(10):611-29.
13. Zavadil J, and Bottinger EP. TGF-beta and epithelial-to-mesenchymal transitions. *Oncogene.* 2005;24(37):5764-74.
14. Kim WS, Park C, Jung YS, Kim HS, Han J, Park CH, Kim K, Kim J, Shim YM, and Park K. Reduced transforming growth factor-beta type II receptor (TGF-beta RII) expression in adenocarcinoma of the lung. *Anticancer Res.* 1999;19(1A):301-6.
15. Kong F, Jirtle RL, Huang DH, Clough RW, and Anscher MS. Plasma transforming growth factor-beta1 level before radiotherapy correlates with long term outcome of patients with lung carcinoma. *Cancer.* 1999;86(9):1712-9.
16. Keshamouni VG, Michailidis G, Grasso CS, Anthwal S, Strahler JR, Walker A, Arenberg DA, Reddy RC, Akulapalli S, Thannickal VJ, et al. Differential protein expression profiling by iTRAQ-2DLC-MS/MS of lung cancer cells undergoing epithelial-mesenchymal transition reveals a migratory/invasive phenotype. *Journal of proteome research.* 2006;5(5):1143-54.

17. Keshamouni VG, Jagtap P, Michailidis G, Strahler JR, Kuick R, Reka AK, Papoulias P, Krishnapuram R, Srirangam A, Standiford TJ, et al. Temporal quantitative proteomics by iTRAQ 2D-LC-MS/MS and corresponding mRNA expression analysis identify post-transcriptional modulation of actin-cytoskeleton regulators during TGF-beta-Induced epithelial-mesenchymal transition. *Journal of proteome research.* 2009;8(1):35-47.
18. Reka AK, Kuick R, Kurapati H, Standiford TJ, Omenn GS, and Keshamouni VG. Identifying inhibitors of epithelial-mesenchymal transition by connectivity map-based systems approach. *J Thorac Oncol.* 2011;6(11):1784-92.
19. Reka AK, Kurapati H, Narala VR, Bommer G, Chen J, Standiford TJ, and Keshamouni VG. Peroxisome proliferator-activated receptor-gamma activation inhibits tumor metastasis by antagonizing Smad3-mediated epithelial-mesenchymal transition. *Mol Cancer Ther.* 2010;9(12):3221-32.
20. Reka AK, Chen G, Jones RC, Amunugama R, Kim S, Karnovsky A, Standiford TJ, Beer DG, Omenn GS, and Keshamouni VG. Epithelial-mesenchymal transition-associated secretory phenotype predicts survival in lung cancer patients. *Carcinogenesis.* 2014;35(6):1292-300.
21. Lamouille S, Xu J, and Derynck R. Molecular mechanisms of epithelial-mesenchymal transition. *Nature reviews Molecular cell biology.* 2014;15(3):178-96.
22. Chockley PJ, and Keshamouni VG. Immunological Consequences of Epithelial-Mesenchymal Transition in Tumor Progression. *Journal of immunology (Baltimore, Md : 1950).* 2016;197(3):691-8.
23. Akalay I, Janji B, Hasmim M, Noman MZ, Andre F, De Cremoux P, Bertheau P, Badoual C, Vielh P, Larsen AK, et al. Epithelial-to-mesenchymal transition and autophagy induction in breast carcinoma promote escape from T-cell-mediated lysis. *Cancer research.* 2013;73(8):2418-27.
24. Kudo-Saito C, Shirako H, Takeuchi T, and Kawakami Y. Cancer metastasis is accelerated through immunosuppression during Snail-induced EMT of cancer cells. *Cancer Cell.* 2009;15(3):195-206.
25. Goswami MT, Reka AK, Kurapati H, Kaza V, Chen J, Standiford TJ, and Keshamouni VG. Regulation of complement-dependent cytotoxicity by TGF-beta-induced epithelial-mesenchymal transition. *Oncogene.* 2016;35(15):1888-98.
26. Kiessling R, Klein E, Pross H, and Wigzell H. "Natural" killer cells in the mouse. II. Cytotoxic cells with specificity for mouse Moloney leukemia cells. Characteristics of the killer cell. *European journal of immunology.* 1975;5(2):117-21.
27. West WH, Cannon GB, Kay HD, Bonnard GD, and Herberman RB. Natural cytotoxic reactivity of human lymphocytes against a myeloid cell line: characterization of effector cells. *Journal of immunology (Baltimore, Md : 1950).* 1977;118(1):355-61.
28. Spits H, Bernink JH, and Lanier L. NK cells and type 1 innate lymphoid cells: partners in host defense. *Nat Immunol.* 2016;17(7):758-64.
29. Imai K, Matsuyama S, Miyake S, Suga K, and Nakachi K. Natural cytotoxic activity of peripheral-blood lymphocytes and cancer incidence: an 11-year follow-up study of a general population. *Lancet.* 2000;356(9244):1795-9.
30. Long EO, Kim HS, Liu D, Peterson ME, and Rajagopalan S. Controlling natural killer cell responses: integration of signals for activation and inhibition. *Annu Rev Immunol.* 2013;31(227-58.
31. Martinet L, and Smyth MJ. Balancing natural killer cell activation through paired receptors. *Nat Rev Immunol.* 2015;15(4):243-54.
32. Schwartzkopff S, Grundemann C, Schweier O, Rosshart S, Karjalainen KE, Becker KF, and Pircher H. Tumor-associated E-cadherin mutations affect binding to the killer cell lectin-like receptor G1 in humans. *Journal of immunology (Baltimore, Md : 1950).* 2007;179(2):1022-9.

33. Boles KS, Barchet W, Diacovo T, Cella M, and Colonna M. The tumor suppressor TSLC1/NECL-2 triggers NK-cell and CD8+ T-cell responses through the cell-surface receptor CRTAM. *Blood.* 2005;106(3):779-86.
34. Kuramochi M, Fukuhara H, Nobukuni T, Kanbe T, Maruyama T, Ghosh HP, Pletcher M, Isomura M, Onizuka M, Kitamura T, et al. TSLC1 is a tumor-suppressor gene in human non-small-cell lung cancer. *Nature genetics.* 2001;27(4):427-30.
35. Murakami Y. Involvement of a cell adhesion molecule, TSLC1/IGSF4, in human oncogenesis. *Cancer science.* 2005;96(9):543-52.
36. Sartor MA, Mahavisno V, Keshamouni VG, Cavalcoli J, Wright Z, Karnovsky A, Kuick R, Jagadish HV, Mirel B, Weymouth T, et al. ConceptGen: a gene set enrichment and gene set relation mapping tool. *Bioinformatics (Oxford, England).* 2010;26(4):456-63.
37. Li C, Ge B, Nicotra M, Stern JN, Kopcow HD, Chen X, and Strominger JL. JNK MAP kinase activation is required for MTOC and granule polarization in NKG2D-mediated NK cell cytotoxicity. *Proceedings of the National Academy of Sciences of the United States of America.* 2008;105(8):3017-22.
38. Kikuchi S, Yamada D, Fukami T, Maruyama T, Ito A, Asamura H, Matsuno Y, Onizuka M, and Murakami Y. Hypermethylation of the TSLC1/IGSF4 promoter is associated with tobacco smoking and a poor prognosis in primary nonsmall cell lung carcinoma. *Cancer.* 2006;106(8):1751-8.
39. Murakami Y. Functional cloning of a tumor suppressor gene, TSLC1, in human non-small cell lung cancer. *Oncogene.* 2002;21(45):6936-48.
40. Heller G, Fong KM, Girard L, Seidl S, End-Pfutzenreuter A, Lang G, Gazdar AF, Minna JD, Zielinski CC, and Zochbauer-Muller S. Expression and methylation pattern of TSLC1 cascade genes in lung carcinomas. *Oncogene.* 2006;25(6):959-68.
41. Shedden K, Taylor JM, Enkemann SA, Tsao MS, Yeatman TJ, Gerald WL, Eschrich S, Jurisica I, Giordano TJ, Misek DE, et al. Gene expression-based survival prediction in lung adenocarcinoma: a multi-site, blinded validation study. *Nat Med.* 2008;14(8):822-7.
42. Gyorffy B, Surowiak P, Budczies J, and Lanczky A. Online survival analysis software to assess the prognostic value of biomarkers using transcriptomic data in non-small-cell lung cancer. *PLoS One.* 2013;8(12):e82241.
43. Gyorffy B, Lanczky A, Eklund AC, Denkert C, Budczies J, Li Q, and Szallasi Z. An online survival analysis tool to rapidly assess the effect of 22,277 genes on breast cancer prognosis using microarray data of 1,809 patients. *Breast Cancer Res Treat.* 2010;123(3):725-31.
44. Keshamouni VG, Michailidis G, Grasso CS, Anthwal S, Strahler JR, Walker A, Arenberg DA, Reddy RC, Akulapalli S, Thannickal VJ, et al. Differential protein expression profiling by iTRAQ-2DLC-MS/MS of lung cancer cells undergoing epithelial-mesenchymal transition reveals a migratory/invasive phenotype. *Journal of proteome research.* 2006;5(5):1143-54.
45. Lopez-Soto A, Huergo-Zapico L, Galvan JA, Rodrigo L, de Herreros AG, Astudillo A, and Gonzalez S. Epithelial-mesenchymal transition induces an antitumor immune response mediated by NKG2D receptor. *Journal of immunology (Baltimore, Md : 1950).* 2013;190(8):4408-19.
46. Lopez-Soto A, Gonzalez S, Smyth MJ, and Galluzzi L. Control of Metastasis by NK Cells. *Cancer Cell.* 2017;32(2):135-54.
47. Malladi S, Macalinao DG, Jin X, He L, Basnet H, Zou Y, de Stanchina E, and Massague J. Metastatic Latency and Immune Evasion through Autocrine Inhibition of WNT. *Cell.* 2016;165(1):45-60.
48. Ghiringhelli F, Menard C, Terme M, Flament C, Taieb J, Chaput N, Puig PE, Novault S, Escudier B, Vivier E, et al. CD4+CD25+ regulatory T cells inhibit natural killer cell functions in a transforming

growth factor-beta-dependent manner. *The Journal of experimental medicine.* 2005;202(8):1075-85.

49. Viel S, Marcais A, Guimaraes FS, Loftus R, Rabilloud J, Grau M, Degouve S, Djebali S, Sanlaville A, Charrier E, et al. TGF-beta inhibits the activation and functions of NK cells by repressing the mTOR pathway. *Sci Signal.* 2016;9(415):ra19.
50. Murakami S, Sakurai-Yageta M, Maruyama T, and Murakami Y. Trans-homophilic interaction of CADM1 activates PI3K by forming a complex with MAGuK-family proteins MPP3 and Dlg. *PLoS One.* 2014;9(2):e82894.
51. Masuda M, Yageta M, Fukuhara H, Kuramochi M, Maruyama T, Nomoto A, and Murakami Y. The tumor suppressor protein TSLC1 is involved in cell-cell adhesion. *The Journal of biological chemistry.* 2002;277(34):31014-9.
52. Faraji F, Pang Y, Walker RC, Nieves Borges R, Yang L, and Hunter KW. Cadm1 is a metastasis susceptibility gene that suppresses metastasis by modifying tumor interaction with the cell-mediated immunity. *PLoS Genet.* 2012;8(9):e1002926.
53. Seong BK, Fathers KE, Hallett R, Yung CK, Stein LD, Mouaaz S, Kee L, Hawkins CE, Irwin MS, and Kaplan DR. A Metastatic Mouse Model Identifies Genes That Regulate Neuroblastoma Metastasis. *Cancer research.* 2017;77(3):696-706.
54. Mao X, Seidlitz E, Truant R, Hitt M, and Ghosh HP. Re-expression of TSLC1 in a non-small-cell lung cancer cell line induces apoptosis and inhibits tumor growth. *Oncogene.* 2004;23(33):5632-42.
55. Henson SM, and Akbar AN. KLRG1--more than a marker for T cell senescence. *Age (Dordr).* 2009;31(4):285-91.
56. Leavy O. T-cell activation: Polarity and CRTAM: a matter of timing. *Nat Rev Immunol.* 2008;8(4):246-.
57. Guillerey C, Huntington ND, and Smyth MJ. Targeting natural killer cells in cancer immunotherapy. *Nat Immunol.* 2016;17(9):1025-36.
58. Leidner R KH, Haddad R, et al. *Society for immunotherapy of cancer (SITC) 31st annual meeting*. National Harbor, MD; November 2016:Abstract 456.

Figure 1

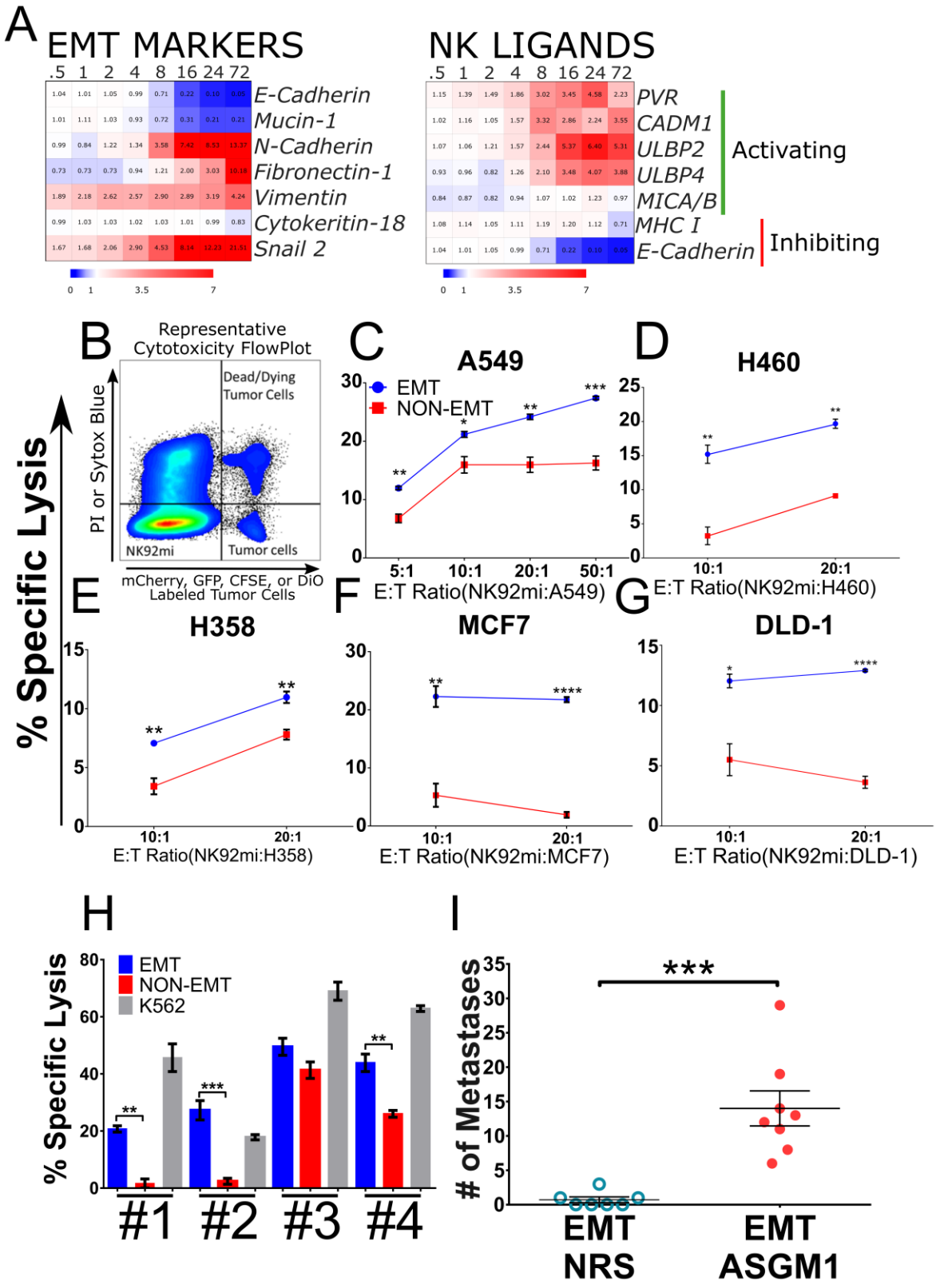
A
EMT MARKERS
.5 1 2 4 8 16 24 72
E-Cadherin
Mucin-1
N-Cadherin
Fibronectin-1
Vimentin
Cytokeritin-18
Snail 2
0 1 3.5 7
NK LIGANDS
.5 1 2 4 8 16 24 72
PVR
CADM1
ULBP2
ULBP4
MICA/B
MHC I
E-Cadherin
Activating
Inhibiting
0 1 3.5 7
B
Representative Cytotoxicity FlowPlot
Dead/Dying Tumor Cells
PI or Sytox Blue
NK92mi
Tumor cells
mCherry, GFP, CFSE, or DiO Labeled Tumor Cells
% Specific Lysis
C
A549
EMT
NON-EMT
5:1 10:1 20:1 50:1
E:T Ratio(NK92mi:A549)
D
H460
10:1 20:1
E:T Ratio(NK92mi:H460)
E
H358
10:1 20:1
E:T Ratio(NK92mi:H358)
F
MCF7
10:1 20:1
E:T Ratio(NK92mi:MCF7)
G
DLD-1
10:1 20:1
E:T Ratio(NK92mi:DLD-1)
H
% Specific Lysis
EMT
NON-EMT
K562
#1 #2 #3 #4
I
# of Metastases
EMT NRS
EMT ASGM1

Figure 1: EMT Differentially Regulates NK Ligands and Promotes Susceptibility to NK-Mediated Cytotoxicity

(**A**) Heat map (blue: down regulation, red: up regulation) representing fold changes, from 0 hrs to 72hrs, time course of differentially expressed EMT markers and NK ligand genes during TGF-β-induced EMT, from previously published gene expression profile data set (GSE17708) (36).

(**B**) Representative flow cytometric plot of cytotoxicity assay showing locations of effector, NK92mi, (fluorophore null cells) and target cells(fluorophore positive) and their exclusion DNA binding dye status(viability indicator).

(**C-G**) NK92mi mediated cytotoxicity plots after 4 hours of co-culture at indicated E:T ratios per cell type and treatment. Cell lines were treated with TGFβ (5ng/ml) for 3, 6, 12, 6, 6 days to induce optimum EMT, as assessed by complete E-cad down regulation and induction of vimentin or N-cadherin, in A549 (**C**), H460 (**D**), H358 (**E**), MCF7 (**F**), and DLD1 (**G**), respectively. Data represents triplicate mean±SEM and two-tailed unpaired, t-tests were performed. All experiments were repeated at least twice.

(**H**) Freshly isolated human peripheral blood derived NK cells were used as effector cells (E:T, 10:1) against A549 cells. K562 cells were used as a positive control for cytotoxicity. Data represents mean±SEM and two-tailed, unpaired, t-tests were performed.

(**I**) To assess experimental metastasis A549 cells were treated with TGFβ (5ng/ml) in vitro and injected through tail vein into $RAG^{-/-}$ mice. After 8 weeks lung were harvested to assess tumor burden. Data shown represents two independent experiment, n=3-4 for each group, and pooled results shown. Error bars are SEM and Mann-Whitney U test was performed, *$P < 0.05$, **$P < 0.01$, ***$P < 0.001$.

Figure 2

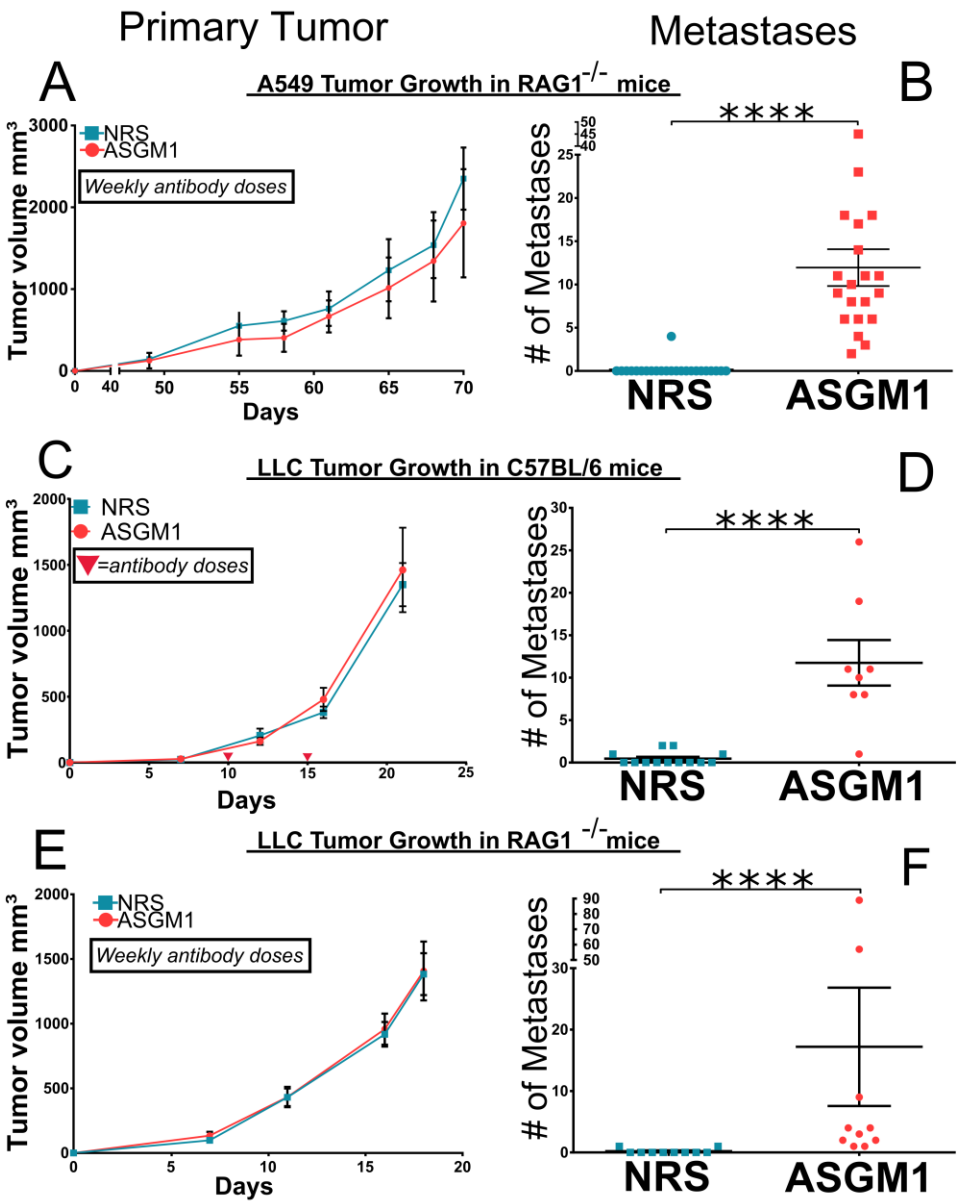

Figure 2: NK Cell Depletion Allows Spontaneous Metastatic Spread without Effecting Primary Tumor Growth.

(**A-F**) To assess the effect of NK cell depletion on primary tumor growth and metastasis indicated cell lines were implanted subcutaneously under the dorsal flanks of RAG1$^{-/-}$ or

C57BL/6 mice. Mice were treated weekly with anti-Asialo GM1 antibody (ASGM1) to deplete NK cells or normal rabbit serum (NRS) as control.

(**A**, **C**, and **E**) Primary tumor growth was monitored and mean-tumor volumes are plotted with errors bars as SEM. Representative data from a single experiment of at least duplicates.

(**B**, **D**, and **F**) Overt lung nodules were counted on the excised lungs to assess spontaneous metastasis. Mouse strains and tumor cell implants are designated. Error bars are SEM and Mann-Whitney U test was performed, *$P < 0.05$, **$P < 0.01$, ***$P < 0.001$. Data represents at least two experiments, n=4-5 per group, and pooled data is shown.

Figure 3

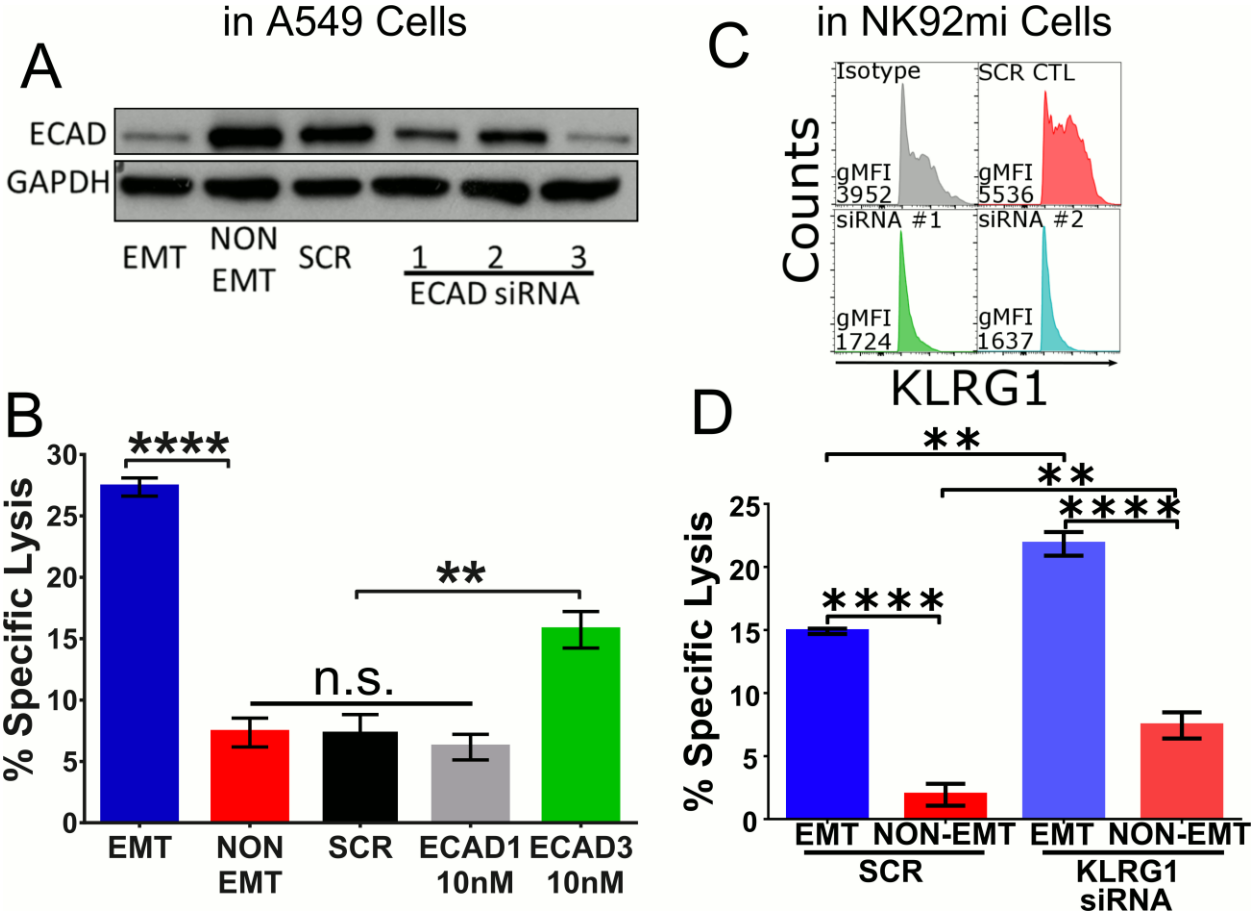

Figure 3: Loss of E-Cadherin Expression Sensitizes Tumor Cells to NK-Mediated Cytotoxicity through KLRG1

(**A**) A549 cells were transfected with 10nM of scrambled (SCR) or 3 different E-cad specific siRNA molecules. After 24hrs, cells were treated with (EMT) or without (NON-EMT) TGF-β (5ng/ml) for 72hrs. E-cad and GAPDH expressions were assessed by western immunoblotting.

(**B**) Susceptibility to NK cytotoxicity was assessed using NK92mi cells as effectors, as described for Figure 1. Mean±SEM is shown and One-Way ANOVA with Tukey's post-hoc analysis was performed *P < 0.05, **P < 0.01, ***P < 0.001.

(**C**) NK92mi cells were transfected with 10 nm of SCR or KLRG1 specific siRNA. After 72hrs, KLRG1 expression was assessed by flow cytometry.

(**D**) NK92mi cells from (**C**) were used as effectors against EMT or non-EMT A549 cells in the NK cytotoxicity assay. Mean±SEM is shown and Two-Way ANOVA with Tukey's post-hoc analysis was performed *P < 0.05, **P < 0.01, ***P < 0.001. All experiments were repeated twice and data shown is representative of one experiment.

Figure 4

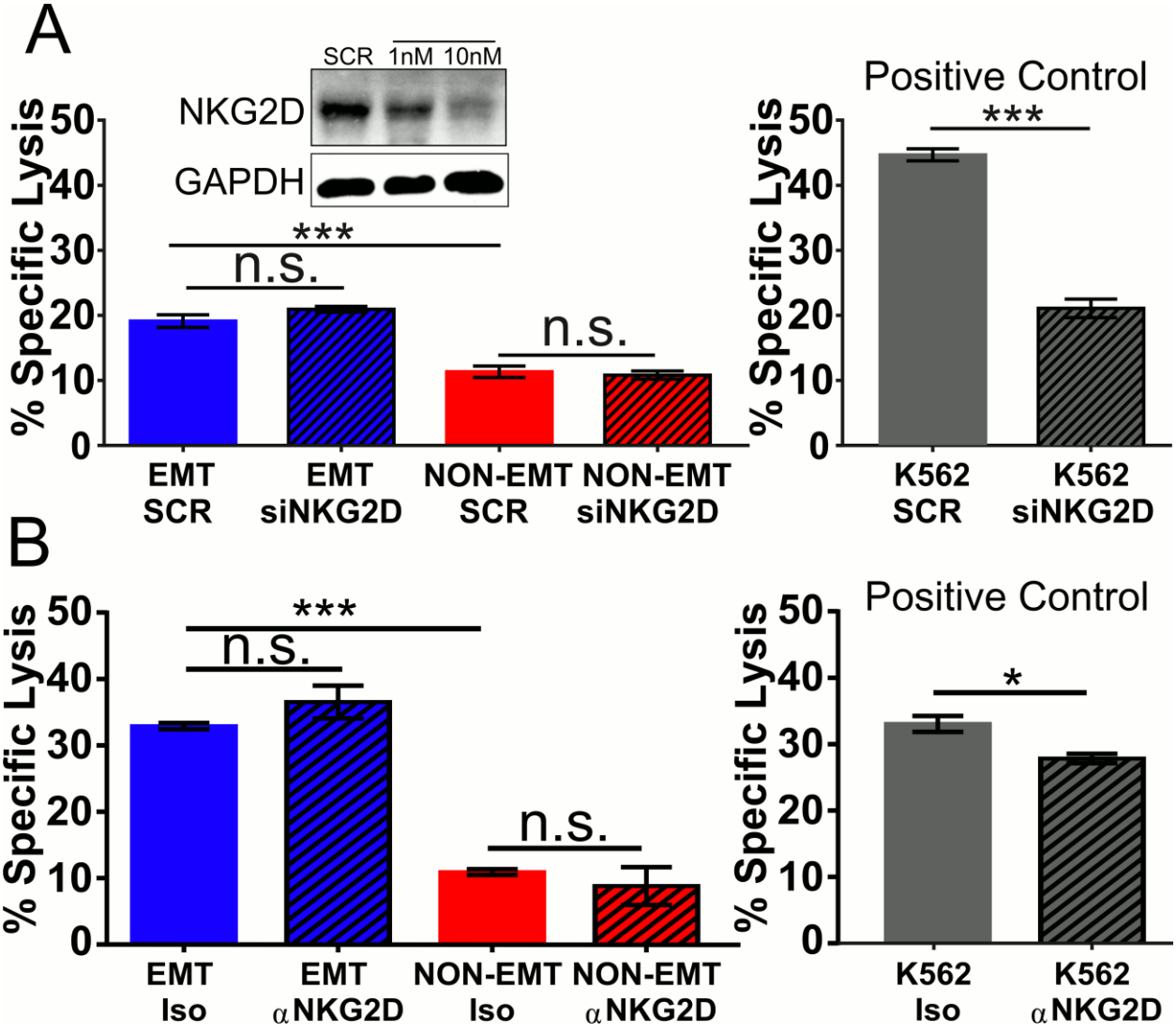

Figure 4: NKG2D Receptor is Not Involved in EMT-Induced Susceptibility to NK-Mediated Cytotoxicity.

(**A**) NK92mi cells were transfected with 10 nm of scrambled (SCR) or NKG2D specific siRNA. After 72 hrs, NKG2D expression was assessed by western immunoblotting (inset), and these cells were used as effectors against A549 cells that are treated with (EMT) or without (Non-EMT) TGF-β (5ng/ml) for 72 hrs, in NK cytotoxicity assay.

(**B**) NKG2D receptors were neutralized by treating NK92mi cells with anti-NKG2D receptor antibody (50 ug/ml) 45 minutes prior to co-culturing them with EMT or non-EMT A549 cells in the NK cytotoxicity assay. All experiments were repeated twice representative data of one experiment shown. Mean±SEM shown and Two-Way ANOVA with Tukey's post-hoc analysis was performed *P < 0.05, **P < 0.01, ***P < 0.001. For Positive Control K562 cytotoxicity, Mean±SEM is shown and two-tailed, unpaired, t-tests were performed *P < 0.05, **P < 0.01, ***P < 0.001.

Figure 5

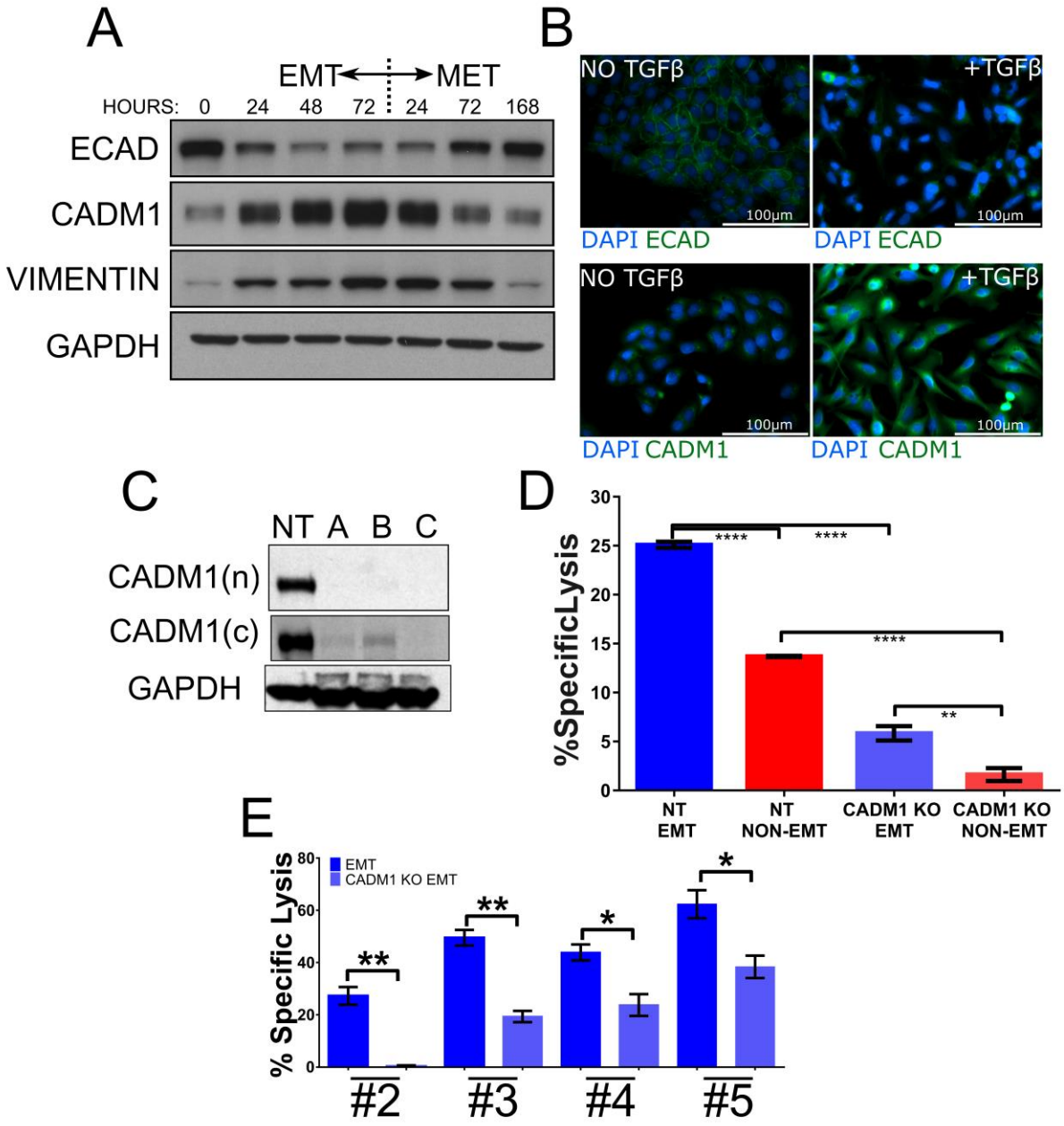

Figure 5: CADM1 Expression is modulated by EMT-MET Cycling and Mediates Tumor Cell Susceptibility to NK Cytotoxicity

(**A**) A549 cells were treated with TGF-β (5 ng/ml) to induce EMT and total proteins were extracted at the indicated times. After 72hrs, cells were washed thrice and replaced with fresh

media to induce MET and total proteins were extracted at the indicated times. Protein expression of E-cad, CADM1, vimentin and GAPDH were assessed by western immunoblotting. (**B**) A549 cells treated with and without TGF-β for 72 h were fixed and assessed for E-cad and CADM1 expression by immunofluorescence staining. Scale bars are 100μM

(**C**) To stably knock-out CADM1, Cas9-expressing A549 cells were transduced with lentivruses expressing three different CADM1 specific CRISPR sgRNA and a non-targeting (NT) control sgRNA. CADM1 knockout was assessed by western immunoblotting using two different CADM1 antibodies raised against C-terminal (CADM1-c) and N-terminal (CADM1-n) portions.

(**D-E**) Susceptibility of CADM1-KO A549 cells to NK cytotoxicity was assessed by co-culturing them with either NK92mi cells or with primary human blood derived NK cells from four different donors. In panel D, Mean±SEM shown and Two-Way ANOVA with Tukey's post-hoc analysis was performed *P < 0.05, **P < 0.01, ***P < 0.001. In panel E, EMT controls are from Figure 1H as these experiments were performed simultaneously. Mean±SEM shown and two-tailed, unpaired, t-tests were performed *P < 0.05, **P < 0.01, ***P < 0.001.

Figure 6

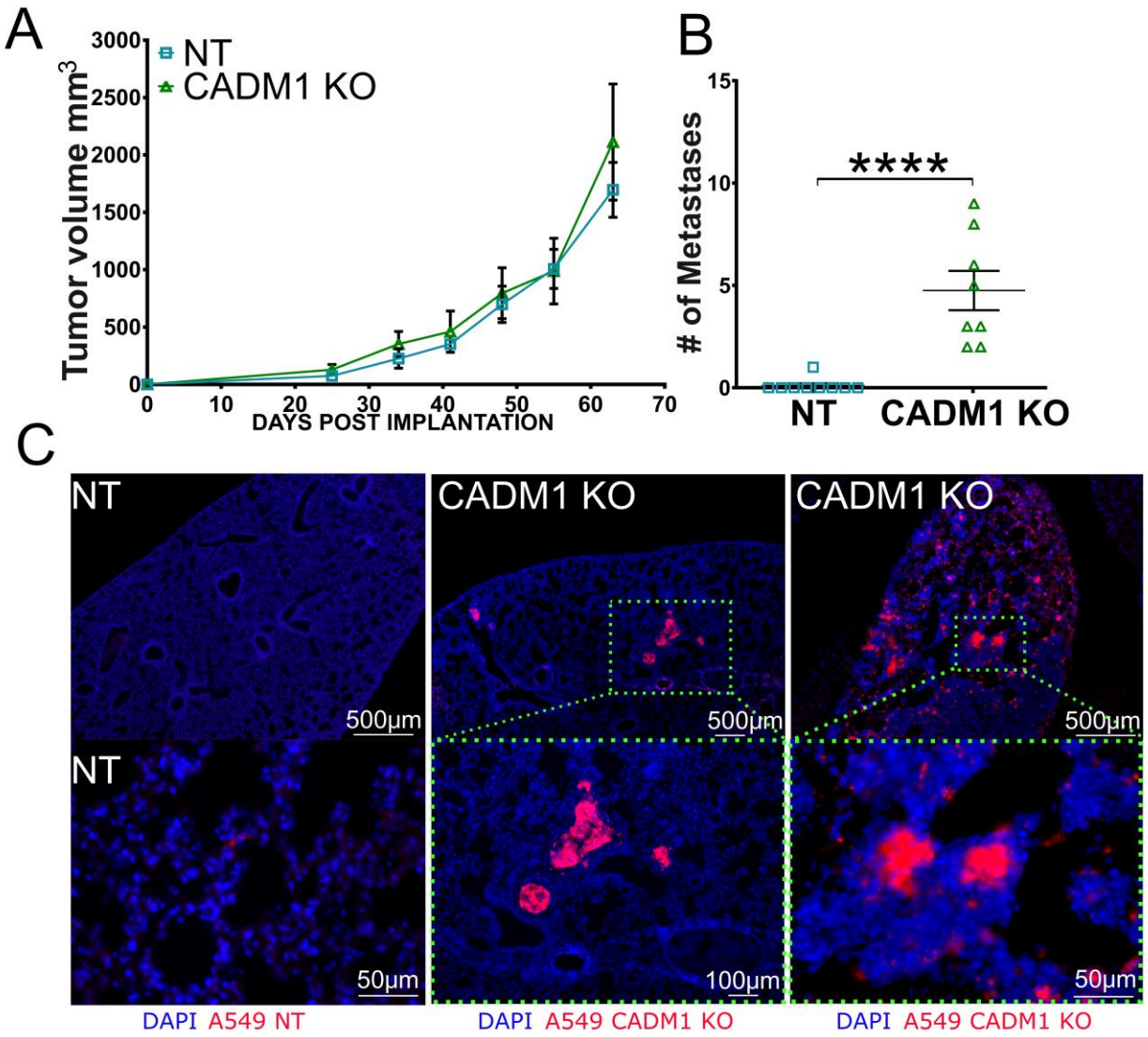

Figure 6: Inhibition of CADM1 in Tumor Cells Allows Spontaneous Metastasis without Effecting Primary Tumor Growth

(**A**) mCherry expressing CADM1 KO and control A549 cells were subcutaneously implanted into the dorsal flanks of RAG1$^{-/-}$ mice. Primary tumor growth was monitored and mean-tumor volumes are plotted, mean±SEM shown. Data is representative of one experiment (n=4-5 mice per group).

(**B**) Overt lung nodules were counted on the excised lungs to assess spontaneous metastasis. Data represents two independent experiments and pooled data is shown, error bars are SEM and Mann-Whitney U test was performed *P < 0.05, **P < 0.01, ***P < 0.001.

(**C**) Presence or lack thereof, of metastatic spread was further confirmed by visualizing mCherry positive tumor cells in the cross-sections of the lungs by immunofluorescence. Top row scale bars are all 500μM and lower row is 50 μM, 100 μM, and 50μM, respectively.

Figure 7

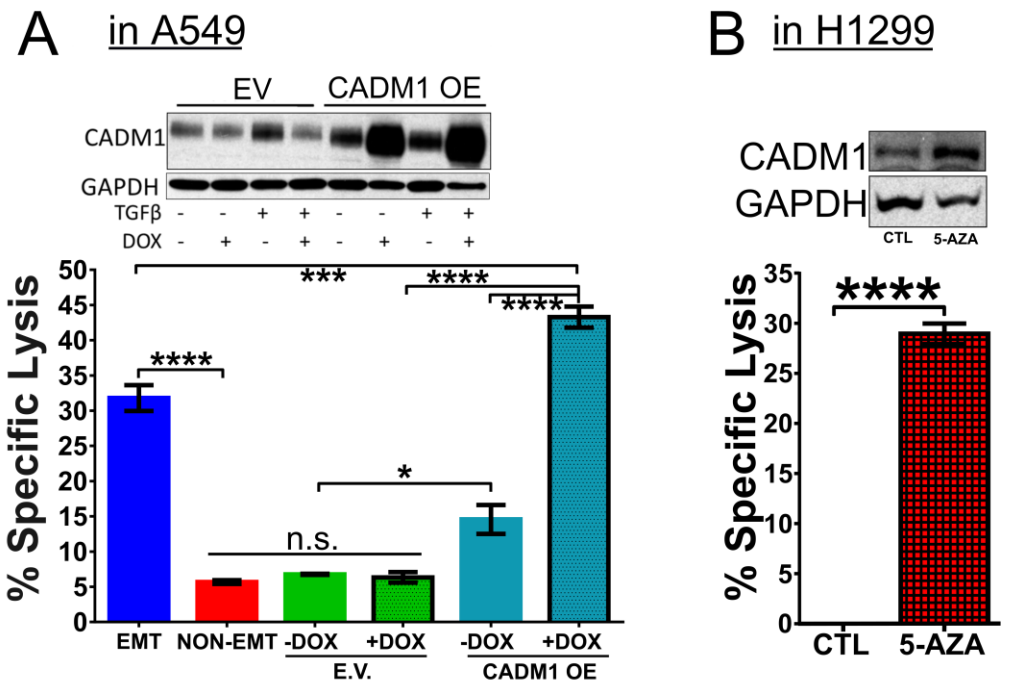

Figure 7: Restoring CADM1 Expression in Tumor Cells is Sufficient to Confer Susceptibility to NK Cytotoxicity

(**A**) Stable A549 cell lines expressing empty vector (E.V.) or vector with doxycycline(DOX)-inducible human CADM1 overexpression (CADM1 OE) were developed. Expression of TGF-β-induced CADM1 was assessed in the presence and absence of doxycycline, by western immunoblotting and susceptibility to NK cytotoxicity was assessed by using NK92mi cells as effectors, as described for figure 1. mean±SEM shown and One-Way ANOVA with Tukey's post-hoc analysis was performed *P < 0.05, **P < 0.01, ***P < 0.001.

(**B**) H1299 cells harboring CADM1 promoter hypermethylation were cultured in the presence and absence of a pan-DNA methylase inhibitor, 5-Azacytidine (5-Aza). CADM1 expression and NK cytotoxicity was assessed as described above. mean±SEM shown and two-tailed, unpaired, t-tests were performed *P < 0.05, **P < 0.01, ***P < 0.001.

Figure 8

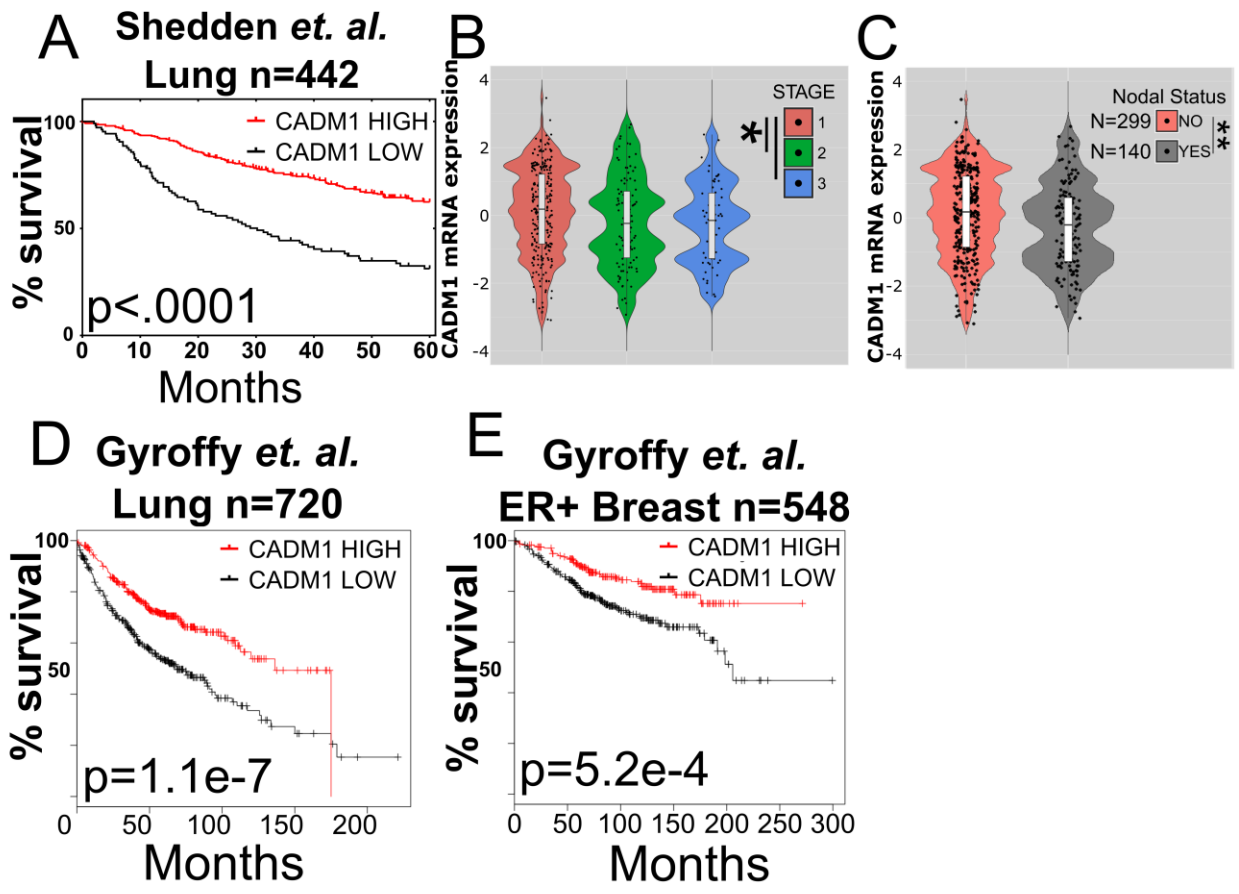

Figure 8: Reduced CADM1 Expression is Correlated to Worse Patient Survival and Metastasis

(**A**) Lung adenocarcinoma patient cohort, Shedden et al.,-lung (n=442), was stratified into low and high CADM1 expressing groups and assessed for overall survival.

(**B** and **C**) Shedden et. al. data set is further classified into sub-groups based on tumor stage and nodal status recorded at the time of diagnosis. Mean CADM1 expression and its distribution are depicted in the violin plots with box and whisker overlays in white. Two-tailed, unpaired, t-tests were performed.

(**D**) Lung adenocarcinoma patient cohort, Gyroffy et al. –lung (n=720), was stratified into low and high CADM1 expressing groups and assessed for overall survival.

(**E**) Breast carcinoma patient cohort, Gyroffy et al.,-ER+ breast (n=548), was stratified into low and high CADM1 expressing groups and assessed for overall survival. (**A,D,** and **E**) Datasets shown here are Kaplan-Meier survival curves with Log-Rank p-values comparing the groups.

Supplemental Figures

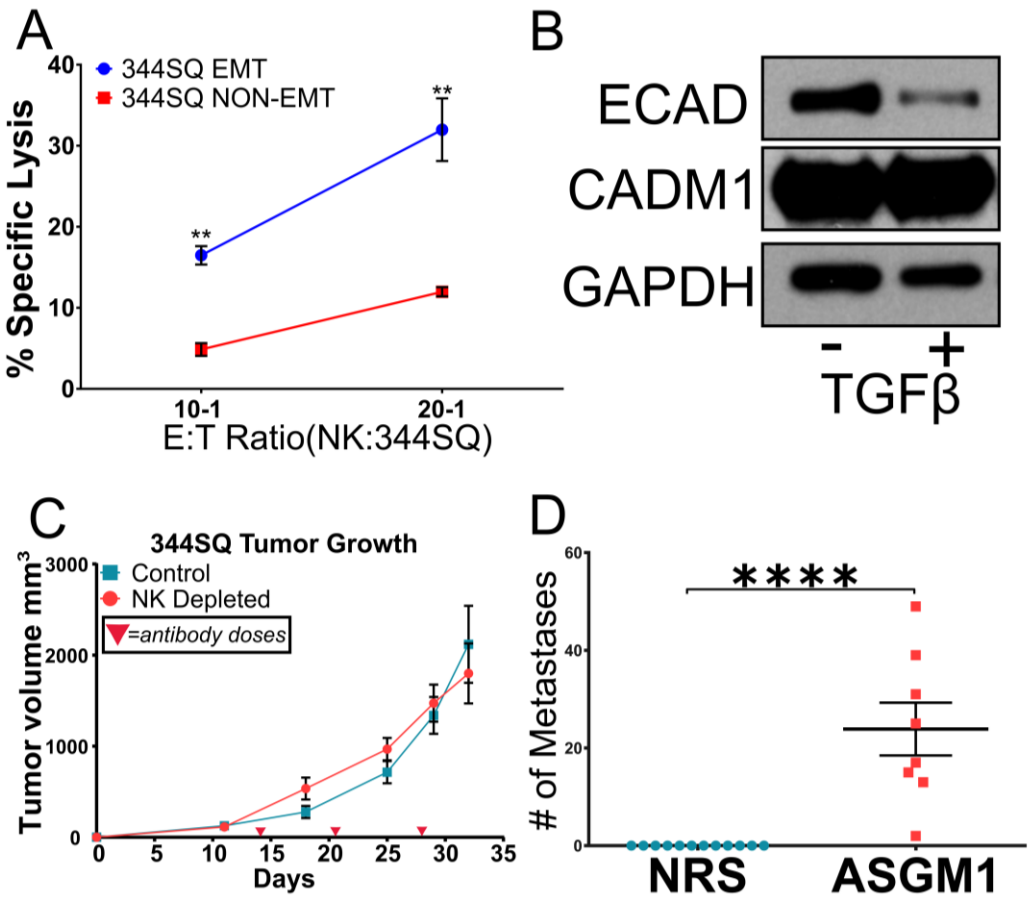

Supplemental Figure 1. EMT-ed Murine 344SQ Cells are Susceptible to NK Mediated Cytotoxicity, Related to Figures 1 and 2

(**A**) To test murine 344SQ lung cancer EMT susceptibility to NK cells, cancer cells were treated with TGFβ for 72 hours and co-cultured with isolated splenic NK cells (CD45+,NK1.1+, CD3e-) from C57BL/6 mice in a cytotoxicity assay as described in Figure 1B. mean±SEM shown, significance was determined by unpaired, two-tailed, t-test.

(**B**) Western immunoblot analysis of ECAD, CADM1, and GAPDH protein levels pre- and post-EMT 344SQ cells.

(**C**) To assess the effect of NK cell depletion on primary tumor growth and metastasis of murine 344SQ tumor cells, cells were implanted subcutaneously into the dorsal flanks of in C57BL/6 mice. Mice were treated with ASGM1 at indicated time points to deplete NK cells. Mean±SEM shown.

(**D**) Overt lung nodules were counted on the excised lungs to assess spontaneous metastasis. Pooled data is shown from two experiments n=4 mice per group. Error bars are SEM and Mann-Whitney U test was performed, *P < 0.05, **P < 0.01, ***P < 0.001.

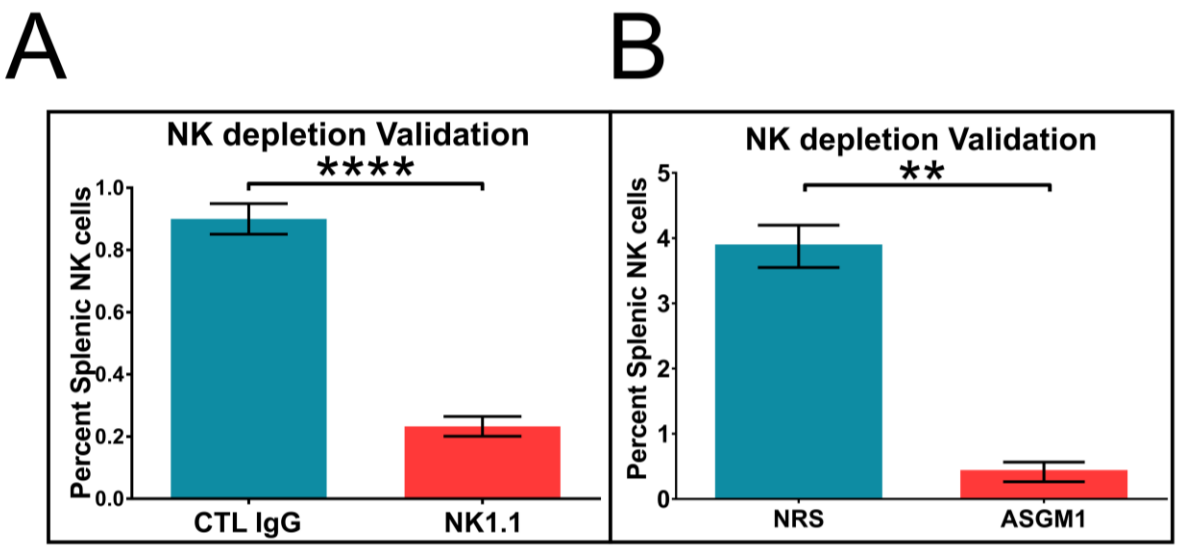

Supplemental Figure 2. NK depletion validation, Related to Figure 2 and Supplemental Figure 3

(**A**) A single injection of 200ug of anti-NK1.1(clone: PK136) or CTL IgG was administered to C57BL/6 mice i.p. and 5 days later spleens were harvested and assessed for NK cells(CD45+,NK1.1+, CD3e-), n=3 per group, mean±SEM is shown.

(**B**) A single injection of 25ul of anti-Asialo GM1(ASGM1) or control normal rabbit serum(NRS) was administered to C57BL/6 RAG1$^{-/-}$ mice and 7 days later spleens were harvested and assessed for NK cells(CD45+,NK1.1+, CD3e-), n=3 per group, mean±SEM is shown. Significance was determined by unpaired, two-tailed, t-test.

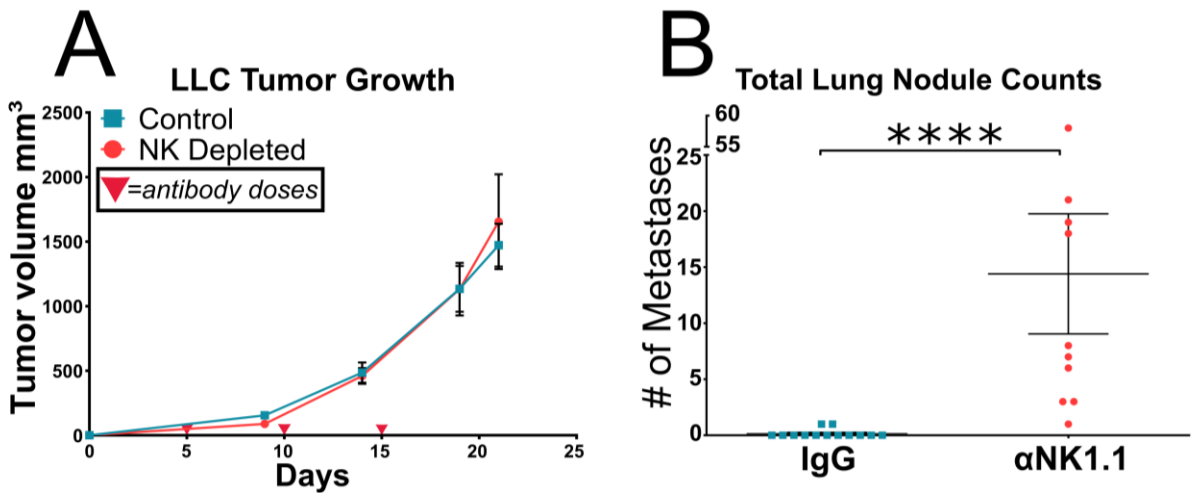

Supplemental Figure 3. LLC Tumors Spontaneously Metastasize with NK Cell Depletion, Related to Figure 2

(**A**) To assess the effect of NK cell depletion on primary tumor growth and metastasis of murine LLC tumor cells, cells were implanted subcutaneously into the dorsal flanks of in C57BL/6 mice. 200μg Anti-NK1.1 was administered every 5 days to deplete NK cells. Mean±SEM shown. See also Supplemental Figure 2.

(**B**) Spontaneous metastatic lung nodules were quantified from (**A**), pooled data from two experiments is shown, n=5 mice per group. Error bars are SEM and Mann-Whitney U test was performed, *P < 0.05, **P < 0.01, ***P < 0.001.

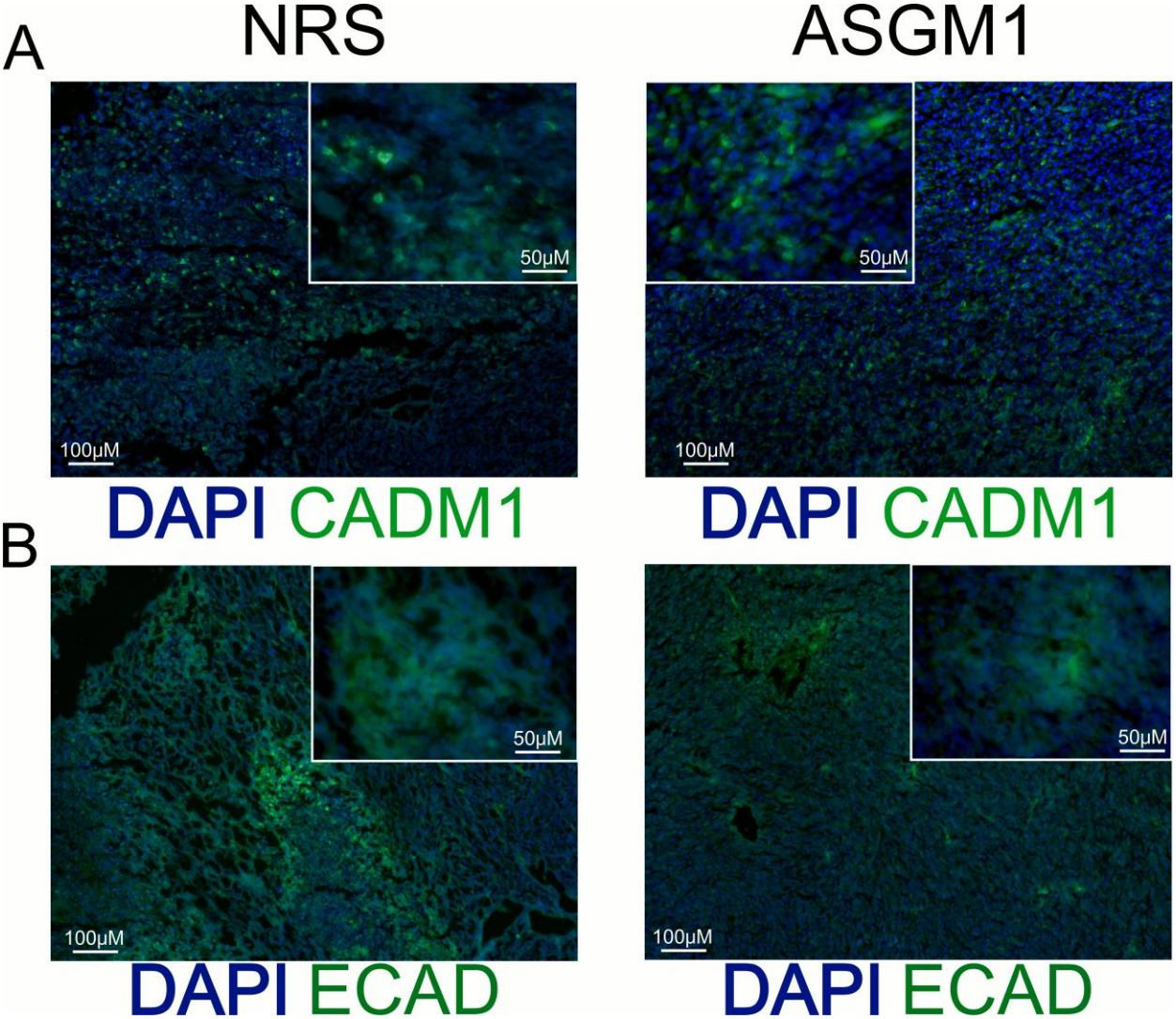

Supplemental Figure 4: CADM1 and E-cad Protein Levels in A549 Tumors in NK depleted and Control mice, Related to Figures 2, 5,

(**A**) A549 tumors grown subcutaneoulsy in RAG1$^{-/-}$ with NK cells depleted (ASGM1) or control (NRS) immunolabeled for CADM1 in green and nuclei were stained with DAPI in blue. Scale bars are 100 micron for large images and 50 micron for insets.

(**B**) Same tumors were immunolabeled for ECAD in green and nuclei were stained with DAPI in blue. Scale bars are 100 micron for large images and 50 micron for insets.

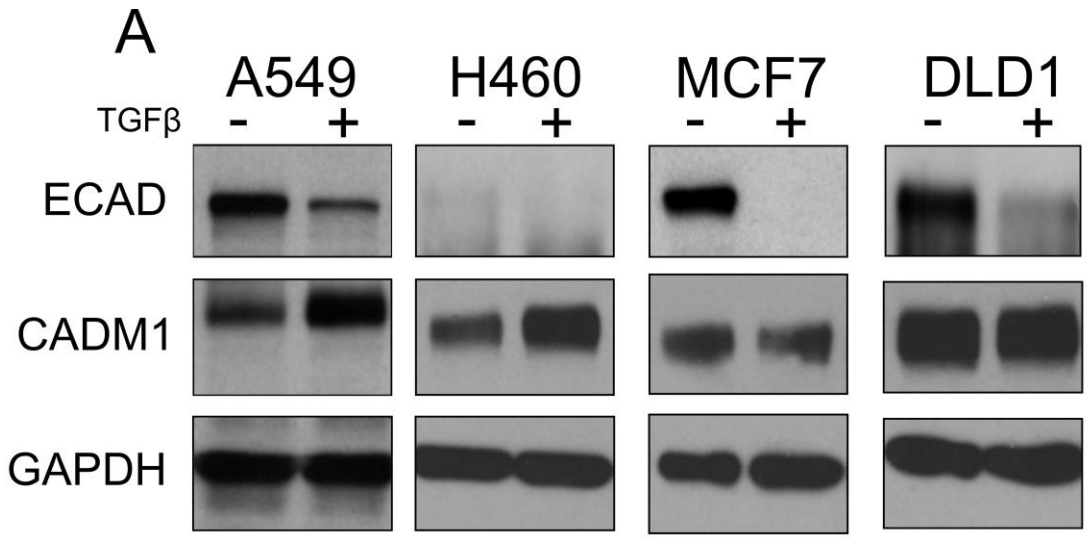

Supplemental Figure 5. CADM1 and ECAD Protein Levels Correlate to EMT-induced Susceptibility to NK Cells, Related to Figures 1 and 5

(**A**) Western immunoblot analysis of ECAD, CADM1, and GAPDH in response to TGFβ after 3 days for A549, and 6 days for MCF7, H460, and DLD1. Immunoblots were cropped for clarity of each cell line used.

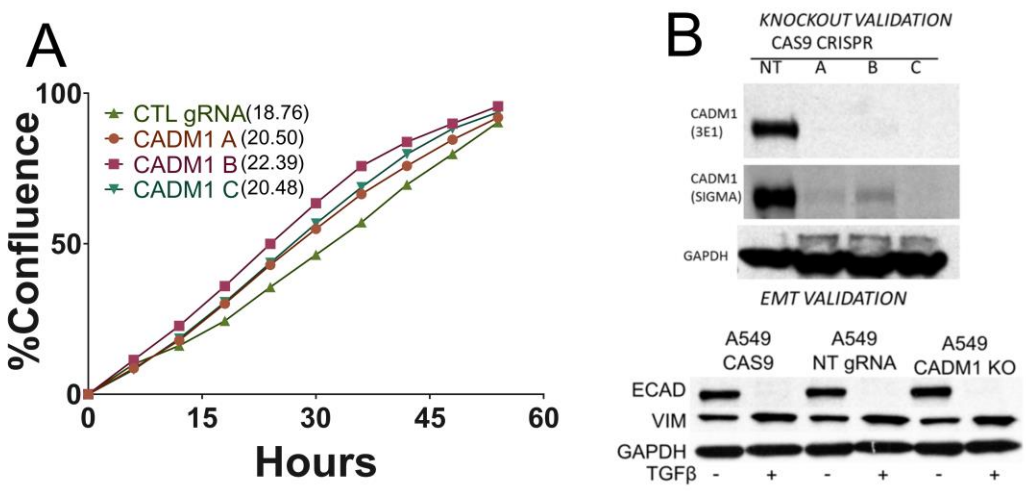

Supplemental Figure 6. CADM1 Deletion Does Not Effect Cell Growth or EMT, Related to Figure 5

(**A**) Confluence percentage as calculated by an Incucyte Imager, EssenBio INC. of A549-CAS9 with indicated signal guide RNAs against CADM1 and a non-targeting (NT) construct. Doubling times were not significantly different, shown in parentheses.

(**B**) Western immunoblot validation of CADM1 deletion utilizing two separate antibodies. 3E1 recognizes the N-Terminal of CADM1 while SIGMA recognizes the C-Terminal domain. Clone C was chosen as our CADM1 KO cell line and TGF-β-induced EMT was validated as seen by ECAD loss and Vimentin (VIM) increases.

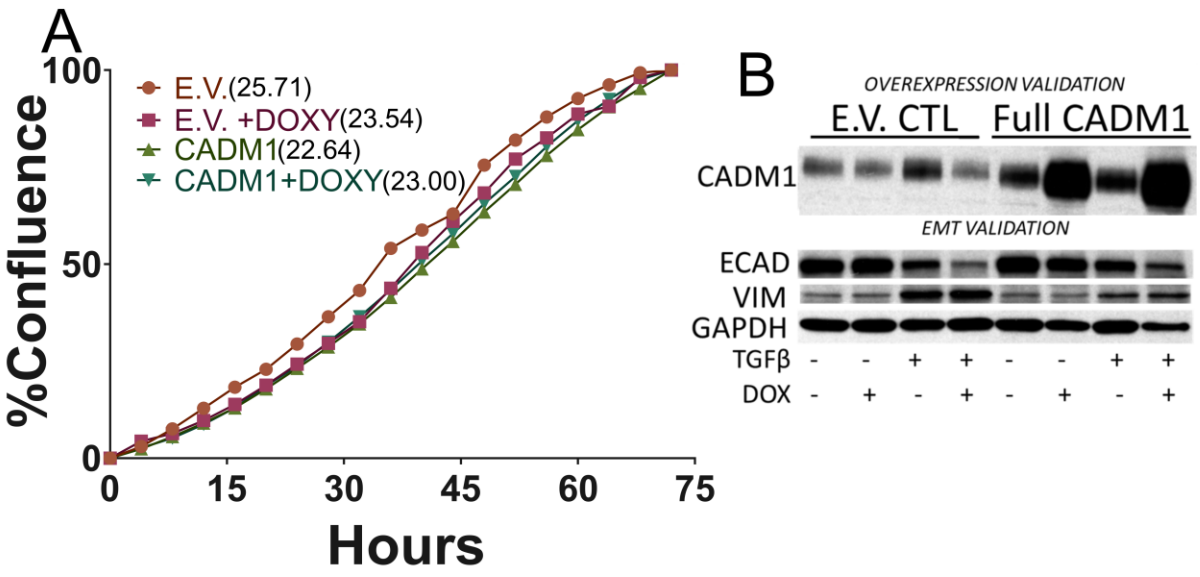

Supplemental Figure 7. CADM1 Overexpression Does Not Effect Cell Growth or EMT, Related to Figure 7

(**A**) Confluence percentage as calculated by an Incucyte Imager, EssenBio INC. of A549 doxycycline-inducible overexpression of CADM1 or with an Empty Vector (E.V.) control. Doubling times were not significantly different shown in parentheses with or without doxycycline or induced CADM1 expression.

(**B**) Western immunoblot validation of CADM1 overexpression and TGF-β-induced EMT was validated as seen by ECAD loss and Vimentin (VIM) increases.

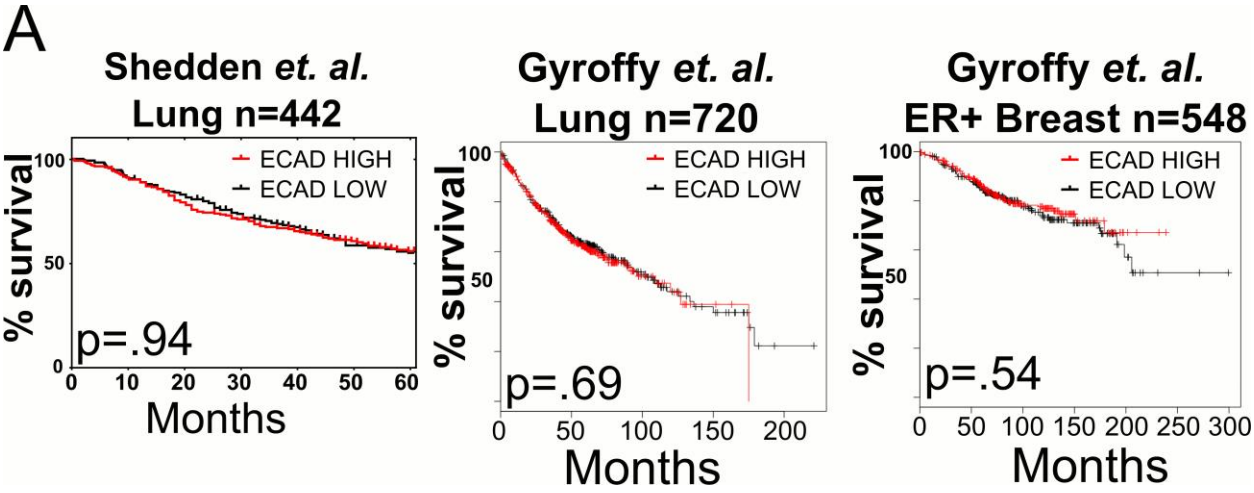

Supplemental Figure 8: E-cadherin expression in Patient Cohorts does not reveal survival benefit, related to Figure 8

(**A**) Lung adenocarcinoma patient cohort, Shedden et al.,-lung (n=442), was stratified into low and high CADM1 expressing groups and assessed for overall survival. Lung adenocarcinoma patient cohort, Gyroffy et al. –lung (n=720), was stratified into low and high CADM1 expressing groups and assessed for overall survival. Breast carcinoma patient cohort, Gyroffy et al.,-ER+ breast (n=548), was stratified into low and high CADM1 expressing groups and assessed for overall survival. Datasets shown here are Kaplan-Meier survival curves with Log-Rank p-values comparing the groups.